FY2022 Master's Degree Thesis

Overlapping Edge Unfoldings for Convex Regular-faced Polyhedrons

Takumi SHIOTA

21677009

Supervisor : Associate Professor Toshiki Saitoh

Division of Systems Design and Informatics
Department of Interdisciplinary Informatics
School of Computer Science and Systems Engineering
Kyushu Institute of Technology

February 2023

Absrtact

Herein, we discuss the existence of overlapping edge unfoldings for convex regular-faced polyhedrons. Horiyama and Shoji showed that there are no overlapping edge unfoldings for all platonic solids and five shapes of Archimedean solids. The remaining five Archimedean solids were also found to have edge unfoldings that overlap. In this study, we propose a method called rotational unfolding to find an overlapping edge unfolding of a polyhedron. We show that all the edge unfoldings of an icosidodecahedron, a rhombitruncated cuboctahedron, an n-gonal Archimedean prism ($3 \leq n \leq 23$), an m-gonal Archimedean antiprism ($3 \leq m \leq 11$), and 48 types of Johnson solids do not overlap. Our algorithm finds overlapping edge unfoldings for a snub cube, and 44 types of Johnson solids. We present analytic proof that an overlapping edge unfolding exists in an n-gonal Archimedean prism ($n \geq 24$), and an m-gonal Archimedean antiprism ($m \geq 12$). Our results prove the existence of overlapping edge unfoldings for convex regular-faced polyhedrons.

Acknowledgements

It is my pleasure to acknowledge the many people who have been the help in writing this thesis. In particular, I would like to thank my principal advisor, Associate Professor Toshiki Saitoh of Kyushu Institute of Technology, for his academic advice in this research. His enthusiastic guidance and support were of great help to me in my research. Despite my immature writing and English skills, I was accepted to a peer-reviewed international conference during my master's program, thanks to his guidance in correcting my writing.

I would also like to thank Professor Eiji Miyano, Associate Professor Akiko Fujimoto, and Assistant Professor Hiroshi Eto of Kyushu Institute of Technology for their various comments on this research and my presentation in the group seminar. They also gave me a lot of advice on application forms for the JSPS Research Fellowship for Young Scientists and others.

I appreciate Professor Ryuhei Uehara, Mr. Tonan Kamata of Japan Advanced Institute of Science and Technology, and Professor Takashi Horiyama of Hokkaido University for their various advice throughout our joint research. I was hosted in their laboratories for a few weeks each, which helped me to broaden my knowledge and discover many open problems.

I am no less grateful to thank all the teachers involved through the AFSA, led by Professor Shinichi Minato of Kyoto University. I am very proud to have been able to participate in the discussions at the AFSA group meetings, even though I am a master's student.

I have indebted to the members of the Kyutech Algorithms Group, including the Competitive Programming Seminar, for following me. Being a lively research group has made my research activities more enjoyable.

Finally, I would like to once again express my deepest gratitude to my family for their constant support.

Contents

List of Figures

List of Tables

Chapter 1

Introduction

The study of unfoldings of polyhedrons is known to have originated from the publication "Underweysung der messung mit dem zirckel un richt scheyt" [3] by Albrecht Dürer in 1525 [4]. Albrecht Dürer drew some edge unfoldings that cut along the edges of a polyhedron and formed the plane's flat polygon. However, all the edge unfoldings are nonoverlapping polygons, i.e., no two faces in the polyhedron exhibit overlapping unfoldings. The following open problem is obtained from this book:

Open Problem 1 ([4], Open Problem 21.1)**.** *Does every convex polyhedron have a nonoverlapping edge unfolding?*

Any convex polyhedron has nonoverlapping unfoldings, i.e., when the polyhedron surface is cut [11, 14]. However, Namiki and Fukuda found a convex polyhedron that has an overlapping edge unfolding [12]. Biedl et al. in 1998 and Grünbaum in 2003 discovered that there exists a nonconvex polyhedron whose every edge unfolding overlaps [1, 6]. Some studies have reported on the existence and/or the number of overlapping edge unfoldings for convex regular-faced polyhedrons. A snub dodecahedron has an overlapping edge unfolding [2]. Horiyama and Shoji presented an algorithm that enumerates overlapping edge unfoldings for a polyhedron. Their algorithm first enumerates edge unfoldings using binary decision diagrams and then checks the overlapping by numerical calculations for each unfolding. They found overlapping edge unfoldings for a truncated dodecahedron, truncated icosahedron, rhombicosidodecahedron, and rhombitruncated icosidodecahedron, as shown in Figure 1.1. In addition, they confirmed that platonic solids and five shapes of Archimedean solids do not have overlapping edge unfoldings [7, 8] (see Table 1.1). The edge unfoldings are represented as spanning trees of a polyhedral graph. The algorithm by Horiyama and Shoji first enumerates the spanning trees to find overlapping edge unfoldings; however, if a polyhedron has an excessive number of spanning trees, it is difficult to enumerate overlapping edge unfoldings even if only a small number of them exist. Thus, they considered isomorphism of unfoldings and enumeration of paths instead of enumeration of the spanning trees to reduce the search space for finding overlapping edge unfolding [7]. However, it remains

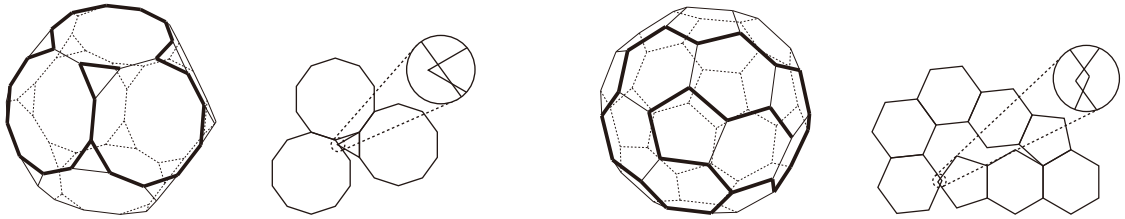

(a) Truncated dodecahedron

(b) Truncated icosahedron

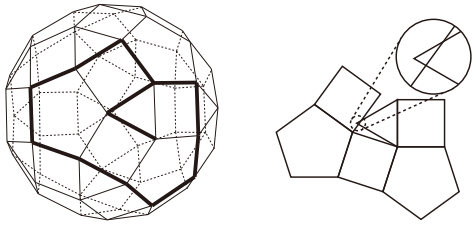

(c) Rhombicosidodecahedron

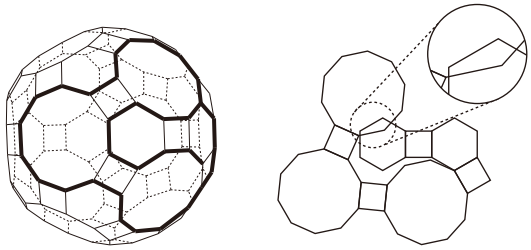

(d) Rhombitruncated icosidodecahedron

Figure 1.1: Examples of overlapping edge unfoldings [8]. The right edge unfolding can be obtained by cutting along the thick line of the left convex polyhedron.

to be clarified a snub cube, an icosidodecahedron, or a rhombitruncated cuboctahedron has overlapping edge unfoldings. Schlickenrieder showed that n-gonal prisms have overlapping edge unfoldings, as shown in Figure 1.2 [13]. However, the side faces of n-gonal prisms are not regular; therefore, the overlapping edge unfoldings for n-gonal Archimedean prisms or n-gonal Archimedean antiprisms have not been studied. It is not clarified Johnson solids have overlapping edge unfoldings. DeSplinter et al. recently studied the edge unfoldings for high-dimensional cubes and showed that a spanning tree of a Roberts graph can represent an edge unfolding [5]. They proposed a rolling and unfolding method, in which the cubes are rotated on a spanning tree and the edges are cut to ensure that they do not overlap.

Our contributions. Herein, we propose a method for determining an overlapping edge unfolding called *rotational unfolding* for a polyhedron. The basic principle of our method is the same as that of the rolling and unfolding method. First, a polyhedron is put on a plane, and the following three steps are performed repeatedly: the bottom edges are cut, the polyhedron is rotated in the plane, and overlapping edge unfoldings are searched. The rolling and unfolding method is suitable for determining edge unfoldings for high-dimensional cubes but not for general shapes. Therefore, we extend the method to n-gon by proposing pruning methods on the rotational unfolding using the distance property and symmetry of a polyhedron to determine overlapping unfoldings

Table 1.1: Existence of an overlapping edge unfolding for platonic solids, Archimedean Solids and (anti)prisms.

Name	Number of edge unfoldings [9]	Is there an overlapping edge unfolding?	Number of overlapping patterns
Tetrahedron	2	No	-
Hexahedron	11	No	-
Octahedron	11	No	-
Dodecahedron	43,380	No [8]	-
Icosahedron	43,380	No [8]	-
Truncated Tetrahedron	261	No [7]	-
Cuboctahedron	6,912	No [7]	-
Truncated hexahedron	675,585	No [7]	-
Truncated octahedron	2,108,512	No [7]	-
Rhombicuboctahedron	6,272,012,000	No [7]	-
Icosidodecahedron	1,741,425,868,800	**No**	-
Snub cube	3,746,001,752,064	**Yes**	**3**
Rhombitruncated cuboctahedron	258,715,122,137,472	**No**	-
Truncated dodecahedron	41,518,828,261,687,500	Yes [8]	**1**
Truncated icosahedron	3,127,432,220,939,473,920	Yes [8]	**2**
Rhombicosidodecahedron	1,679,590,540,992,923,166,257,971,200	Yes [8]	Open
Snub dodecahedron	7,303,354,923,116,108,380,042,995,304,896,000	Yes [2]	Open
Rhombitruncated icosidodecahedron	181,577,189,197,376,045,928,994,520,239,942,164,480	Yes [8]	Open
n-gonal Archimedean prism	$\begin{cases} \frac{1}{8\sqrt{3}}\{2\sqrt{3}n+\sqrt{3}(2+\sqrt{3})^n & \\ \quad +(2+\sqrt{3})^{\lfloor\frac{n}{2}\rfloor}(4+2\sqrt{3}) & (\text{if } n \text{ is odd}) \\ \quad +(2-\sqrt{3})^{\lfloor\frac{n}{2}\rfloor}(2\sqrt{3}-4) & \\ \quad +\sqrt{3}((2-\sqrt{3})^n-2)\} & \\ 11 & (\text{if } n=4) \\ \frac{1}{24}\{3(2+\sqrt{3})^n+4\sqrt{3}(2+\sqrt{3})^{\frac{n}{2}} & \\ \quad +3(2-\sqrt{3})^n-4\sqrt{3}(2-\sqrt{3})^{\frac{n}{2}} & (\text{otherwise}) \\ \quad +6n-6\} & \end{cases}$	**No** (**if** $3 \le n \le 23$) **Yes** (**if** $n \ge 24$)	Open
n-gonal Archimedean antiprism	$\begin{cases} 11 & (\text{if } n=3) \\ \frac{1}{10}\left\{\left(\frac{1+\sqrt{5}}{2}\right)^{4n}+\left(\frac{1+\sqrt{5}}{2}\right)^{-4n}-2\right\} & \\ \quad +\frac{(3+\sqrt{5})^n-(3-\sqrt{5})^n}{2^{n+1}\sqrt{5}} & (\text{otherwise}) \end{cases}$	**No** (**if** $3 \le n \le 11$) **Yes** (**if** $n \ge 12$)	Open

efficiently. As a result, we obtain the following:

- We show that all the edge unfoldings of an icosidodecahedron and a rhombitruncated cuboctahedron do not overlap and that a snub cube has only three types of overlapping edge unfoldings, as shown in Figure 1.3, with two vertices of faces in contact with each other. These are indicated in bold in Table 1.1. These results are used to the determine the existence of overlapping edge unfoldings for Archimedean solids.

- We find a new type of overlapping edge unfoldings for a truncated icosahedron, as shown in Figure 1.4, and show that only one and two types of edge unfoldings exist in a truncated dodecahedron and truncated icosahedron, respectively.

- We show that 48 Johnson solids do not have overlapping edge unfoldings and 44 Johnson solids have overlapping edge unfoldings, as shown in Table 1.2. For 20 solids in the 44 Johnson solids which have overlapping edge unfoldings, we

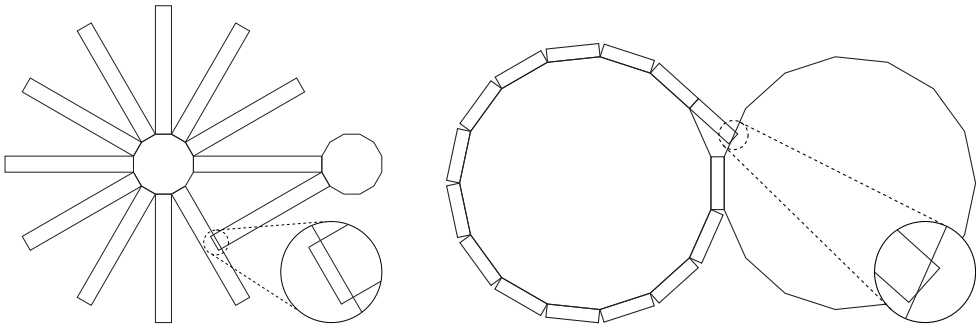

Figure 1.2: Overlapping edge unfoldings for an n-gonal prisms [13].

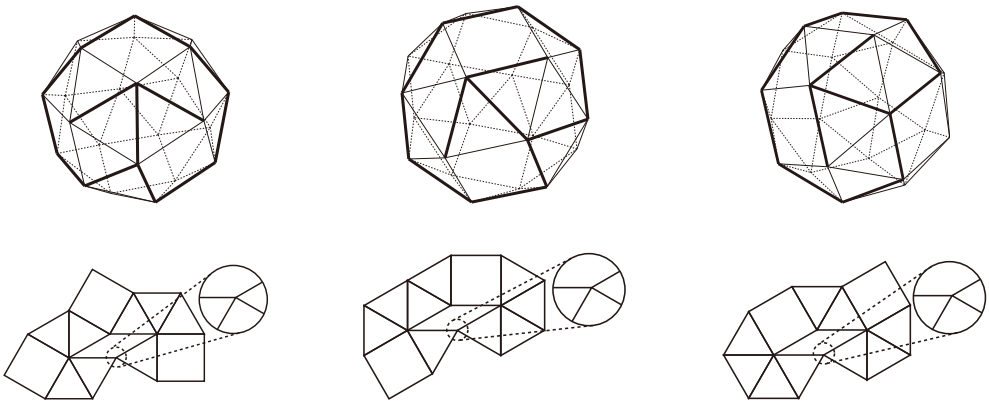

Figure 1.3: Three types of edge unfoldings have two faces in contact with the snub cube. The edge unfolding can be obtained by cutting each snub cube along the thick line.

enumerate the overlapping patterns. We find some edge unfoldings in Johnson solids with two vertices of faces, the edge of one face and the vertex of the other face, or two edges of faces in contact with each other.

- Through rotational unfolding, we show that overlapping edge unfoldings do not exist for n-gonal Archimedean prisms and m-gonal Archimedean anti-prisms for $3 \leq n \leq 23$ and $3 \leq m \leq 11$ by rotational unfolding. We also demonstrate that overlapping edge unfoldings exist in n-gonal Archimedean prisms and m-gonal Archimedean antiprisms for $n \geq 24$ and $m \geq 12$, as shown in Figure 1.5.

Our results prove the existence of overlapping edge unfoldings for convex regular-faced polyhedrons.

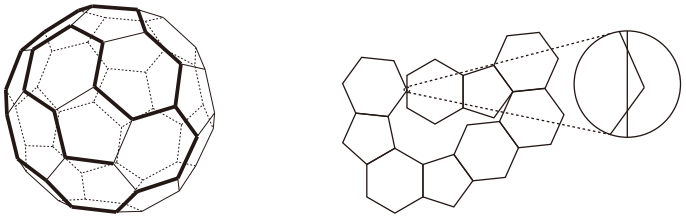

Figure 1.4: A new overlapping edge unfolding in a truncated icosahedron. The right edge unfolding is obtained by cutting along the thick line of the left convex polyhedron.

Table 1.2: Existence of an overlapping edge unfolding for Johnson solids.

Name	Number of edge unfoldings [9]	Is there an overlapping edge unfolding?	Number of overlapping patterns	Name	Number of edge unfoldings [9]	Is there an overlapping edge unfolding?	Number of overlapping patterns
J1	8	No	-	J47	1,864,897,711,733,918,792	Yes	Open
J2	15	No	-	J48	267,015,959,942,030,583,130	Yes	Open
J3	308	No	-	J49	173	No	-
J4	3,030	No	-	J50	1,401	No	-
J5	29,757	No	-	J51	3,549	No	-
J6	7,825,005	No	-	J52	4,201	No	-
J7	63	No	-	J53	38,526	No	-
J8	448	No	-	J54	19,035	Yes	**1**
J9	3,116	No	-	J55	88,776	Yes	**1**
J10	3,421	No	-	J56	176,967	Yes	**1**
J11	40,321	No	-	J57	544,680	Yes	**1**
J12	9	No	-	J58	9,272,497	Yes	**1**
J13	99	No	-	J59	82,580,526	Yes	**1**
J14	156	No	-	J60	410,335,964	Yes	**1**
J15	2,010	No	-	J61	4,790,966,400	Yes	**1**
J16	25,574	No	-	J62	7,050	No	-
J17	13,041	No	-	J63	289	No	-
J18	268,260	No	-	J64	1,409	No	-
J19	28,427,091	No	-	J65	207,576	No	-
J20	2,982,139,245	Yes	**4**	J66	6,865,163,910	Yes	**13**
J21	822,310,337,549	Yes	**9**	J67	5,685,916,514,256	Yes	**13**
J22	6,193,152	No	-	J68	6,849,584,355,849,548,062,500	Yes	Open
J23	1,935,360,000	No	-	J69	46,849,407,942,992,327,926,343,838	Yes	Open
J24	599,660,087,082	Yes	**6**	J70	232,575,882,499,181,854,544,317,560	Yes	Open
J25	170,242,287,969,600	Yes	Open	J71	2,079,942,317,394,110,986,896,181,956,672	Yes	Open
J26	152	No	-	J72	20,668,673,558,050,742,614,946,330,896	Yes	Open
J27	27,195	No	-	J73	10,597,511,106,353.370,064,654,696,448	Yes	Open
J28	1,867,560	No	-	J74	52,898,913,344,353,749,804,959,881,152	Yes	Open
J29	1,934,427	No	-	J75	36,042,636,312,577,358,126,529,767,936	Yes	Open
J30	125,939,163	No	-	J76	2,108,152,090,439,487,210,452,928	Yes	Open
J31	132,627,603	No	-	J77	2,163,545,802,723,460,484,299,200	Yes	Open
J32	69,953,702,412	Yes	**2**	J78	10,819,092,174,083,407,318,469,376	Yes	Open
J33	74,520,844,992	Yes	**2**	J79	11,085,623,675,648,531,139,403,888	Yes	Open
J34	9,650,165,403,136	Yes	**1**	J80	108,182,283,486,496,129,152	Yes	Open
J35	25,158,925	No	-	J81	523,563,323,531,253,902,848	Yes	Open
J36	25,203,000	No	-	J82	1,075,622,906,381,856,553,376	Yes	Open
J37	18,874,379,520	No	-	J83	32,858,151,465,900,184	Yes	Open
J38	13,537,250,963,730	Yes	**4**	J84	1,109	No	-
J39	13,601,327,004,000	Yes	**4**	J85	80,742,129	No	-
J40	7,537,820,216,388,070	Yes	Open	J86	21,204	No	-
J41	7,580,441,138,131,750	Yes	Open	J87	326,423	No	-
J42	1,048,493,264,659,994,295	Yes	Open	J88	500,959	No	-
J43	1,055,767,519,017,973,725	Yes	Open	J89	8,094,150	No	-
J44	882,609,105	Yes	**4**	J90	64,950,268	No	-
J45	1,721,235	Yes	**6**	J91	108,936	No	-
J46	3,254,364,517,723,165	Yes	Open	J92	39,287,808	No	-

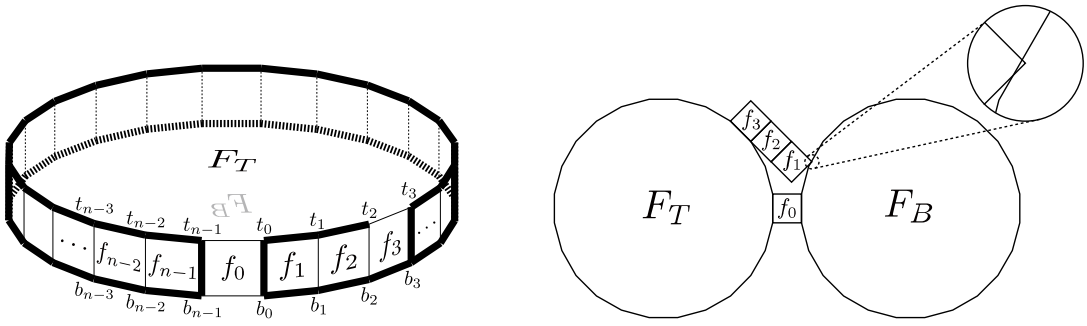

(a) 24-gonal Archimedean prism

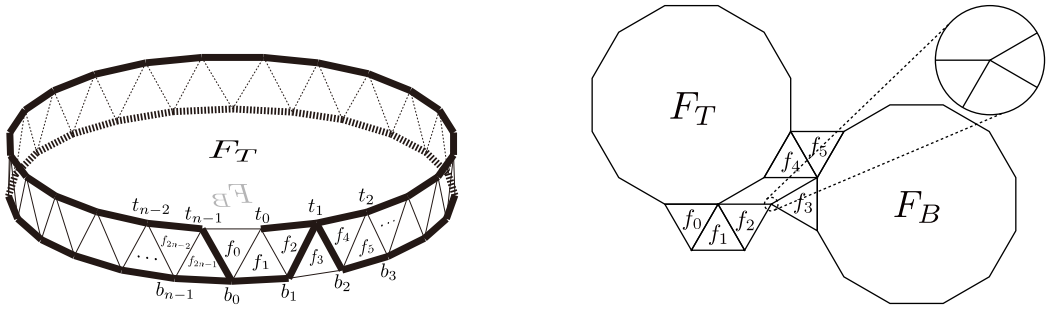

(b) 12-gonal Archimedean anti-prism

Figure 1.5: An overlapping edge unfolding in an n-gonal Archimedean (anti-)prism. The right edge unfolding is obtained by cutting along the thick line of the left convex polyhedron.

Chapter 2

Preliminaries

Let $G = (V, E)$ be a simple graph where V is a set of vertices and $E \subseteq V \times V$ is a set of edges. A sequence of vertices $(v_1, \ldots, v_k)$ is a *path* if all vertices in the sequence are distinct and every consecutive two vertices are adjacent. A graph is *connected* if there exists a path between any two vertices of the graph. If a graph $T = (V_T, E_T)$ is connected and $|E_T| = |V_T| - 1$, the graph is called a *tree*. A tree $T = (V_T, E_T)$ is a *spanning tree* of $G = (V, E)$ if $V_T = V$ and $E_T \subseteq E$.

A *polyhedron* is a three-dimensional object consisting of at least four polygons, called *faces*, joined at their edges. A *convex polyhedron* is a polyhedron with the interior angles of all two faces less than π. A *convex regular-faced polyhedron* is a convex polyhedron with all faces are regular polygon. A *Platonic solid* is a convex regular-faced polyhedron with faces composed of congruent regular polygons. An n *prism* is a polyhedron composed of two identical n-sided polygons, called *bases*, facing each other, and n parallelograms, called *side faces*, connecting the corresponding edges of the two bases. An n *antiprism* is a polyhedron composed of two bases of congruent n-sided polygons and $2n$-sided alternating triangles. An *n-gonal (anti)prism* is an n (anti)prism if the bases are n-sided regular polygons and an *n-gonal Archimedean (anti)prism* is an n-gonal (anti)prism if it is a convex regular-faced polyhedron (i.e., the side faces are also regular). An *Archimedean solid* is a convex regular-faced polyhedron composed of regular polygons with the same type and order of regular polygons gathered at the vertices, except Platonic solids, and Archimedean (anti)prisms. A *Johnson solid* is a convex regular-faced polyhedron, except Platonic solids, Archimedean solids, and Archimedean (anti)prisms. It is known that there are 92 Johnson solids [10].

Let P be a polyhedron. P can be viewed as a graph $G_P = (V_P, E_P)$, where V_P is a set of vertices and E_P is a set of edges of P. An *unfolding* (also called a net, a development, or a general unfolding) of the polyhedron P is a flat polygon formed by cutting P's edges or faces and unfolding it into a plane. An edge unfolding of P is an unfolding formed by cutting only edges. We have the following lemma for an edge unfolding of P.

Lemma 1 (see e.g., [4], Lemma 22.1.1)**.** *The cut edges of an edge unfolding of P form*

a spanning tree of G_P.

This lemma implies that a spanning tree of G_P corresponds to an edge unfolding of P. Two faces in P are *neighbors* if they contain a common edge. A *dual graph* of P is a graph where each vertex of the dual graph corresponds to a face in the polyhedron, and two vertices are adjacent if and only if the corresponding two faces are neighbors. A spanning tree of the dual graph of P can also be considered an edge unfolding [13].

The following proposition is used to determine whether an edge unfolding of a polyhedron P is overlapping.

Proposition 1 ([8])**.** *If for any two faces in an edge unfolding, the circumscribed circles of the two faces do not overlap, then the edge unfolding is not overlapping.*

This proposition is useful for efficiently checking the overlapping of an edge unfolding, and it is a necessary condition for overlapping edge unfoldings. If the circumscribed circles of two faces of P intersect, we use numerical calculations to check the overlapping.

Chapter 3

Rotational unfolding

In this section, we propose an algorithm for detecting overlapping edge unfoldings for a polyhedron P. A spanning tree $T(U)$ of a dual graph $D(P)$ of P represents an edge unfolding U. We can determine all overlapping edge unfoldings by enumerating all spanning trees of $D(P)$ and then check the overlapping of the corresponding unfoldings. However, a polyhedron generally contains a large number of spanning trees. Our algorithm employs Lemma 2 to enumerate the paths rather than the spanning trees to efficiently search for overlapping edge unfoldings.

Lemma 2 ([5,7])**.** *Let U be an overlapping edge unfolding of a polyhedron P, and $T(U)$ be a spanning tree corresponding to U of the dual graph $D(P)$. There exist two vertices $v, v' \in T(U)$ such that a path from v to v' in $T(U)$ represents a consecutive sequence of faces in U with overlapping the two faces corresponding to v and v'.*

For a polyhedron P, we present a simple and recursive procedure called rotational unfolding to find paths and check their overlap. In this procedure, we first place P in the plane. The *start face* f_s of P is the bottom face. We rotate P and unfold the current bottom in the rotational unfolding. Let f_ℓ be the current bottom face, called the *last face*. In the first step of the procedure, f_ℓ is the start face f_s. The rotational unfolding first checks whether there exists a neighbor face of f_ℓ in P. Then, for each neighbor face f, we run the following three steps: we cut the edges of f_ℓ except for the edge sharing f, roll the polyhedron P to be the bottom f, and check the overlap between f_s and f. To check the overlapping of edge unfoldings, we compute the coordinate of the outer center of f from that of f_ℓ and the angle of the shared edge. Then, we check the overlap between f_s and f using Proposition 1 or numerical calculations. Let v_{f_s} and v_f be the vertices corresponding to the face f_s and f of $D(P)$, respectively. If f_s and f overlap, we output a part of edge unfolding corresponding to a path from v_{f_s} to v_f. Otherwise, we run the procedure recursively. Figure 3.1 illustrates the rotational unfolding procedure.

Although the number of paths is smaller than that of spanning trees, it is still large. To reduce the search space, we implement three methods for speeding up the search.

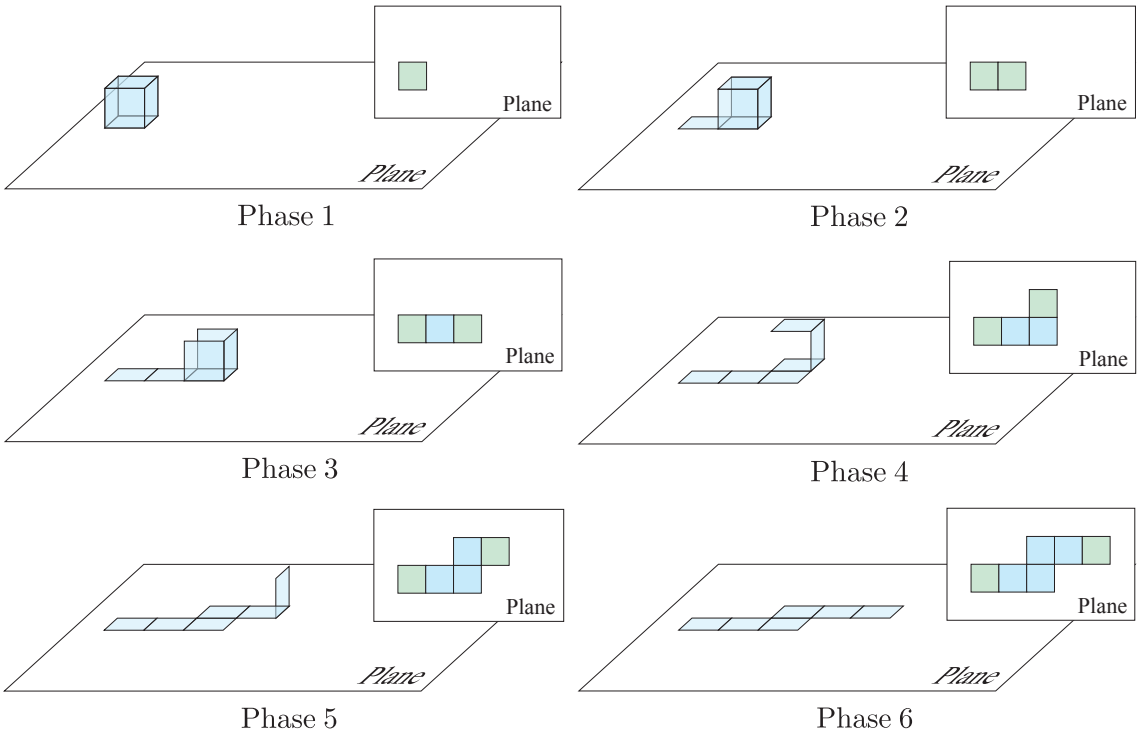

Figure 3.1: Illustration of rotational unfolding.

The first method uses the simple distance property. Let D be the Euclidean distance between the outer center of f_s and that of f, r_s and r be the circumscribed circle radii of f_s and f, respectively, and W be the sum of circumscribed circle diameters of the remaining faces in P. For f_s and a face in P to overlap, the distance between f_s and f have to be smaller than W; that is, if $W + r_s + r < D$, f_s does not overlap any other faces in P for any unfolding because f_s is too far from the other faces in P. Thus, if $W + r_s + r < D$, we prune the search.

The second method uses the symmetry of the polyhedron. Figure 3.2 shows a symmetric edge unfolding. If a polyhedron has such symmetric unfoldings, we only compute one of them to check if a self-overlapping edge unfolding exists. To implement this pruning, we maintain the y-coordinate of the outer center of the last face before it becomes non-zero. We prune the search if the y-coordinate becomes negative for the first time. Note that, this pruning does not work for a snub cube, a snub dodecahedron and Johnson solids because they do not have a mirror symmetry.

In the third method, we run the rotational unfolding by fixing a few steps of the search. In the algorithm, we first choose a start face. We only need to consider restricted patterns of the first few faces of polyhedrons. For example, in the case of a truncated tetrahedron, which consists of regular triangles and regular hexagons, as shown in Figure 3.3, we only consider three patterns of the start and next face pairs: (a) a triangle and a hexagon, (b) a hexagon and a triangle, and (c) a hexagon and a hexagon.

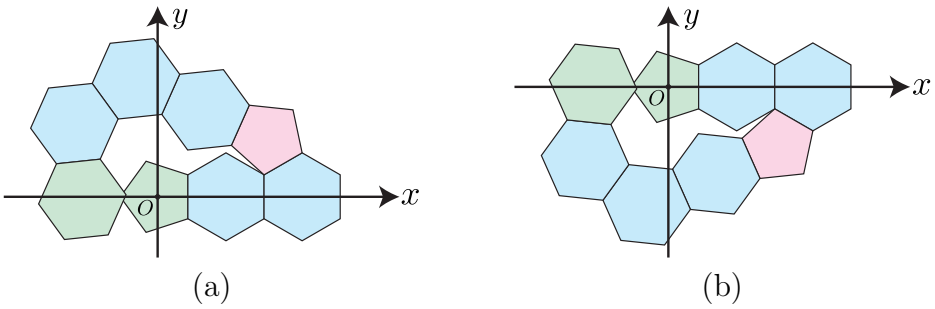

Figure 3.2: (a) and (b) are symmetric with respect to the $x-$axis.

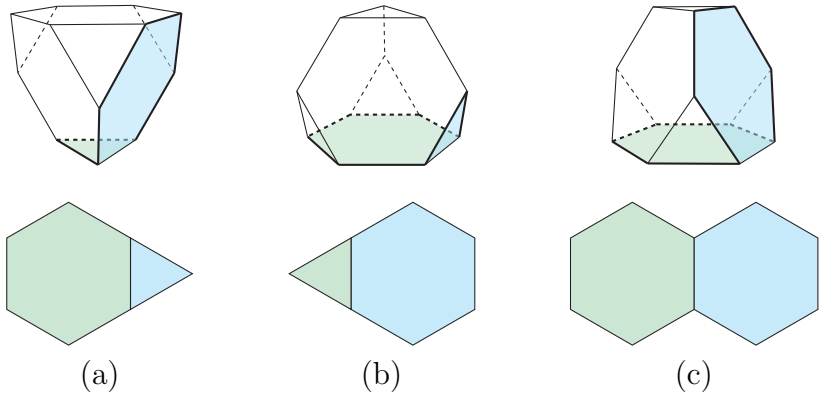

Figure 3.3: Cases of the first two faces in the rotational unfolding.

We find paths from these patterns as start faces. Note that we cannot consider only the first face shape to find the patterns. For example, both of the start faces of Figure 3.4 (a) and (b) are squares; however, we need to consider both cases because the remaining polyhedrons are not isomorphic. Thus, for each polyhedron shape, we have to find start patterns based on symmetry.

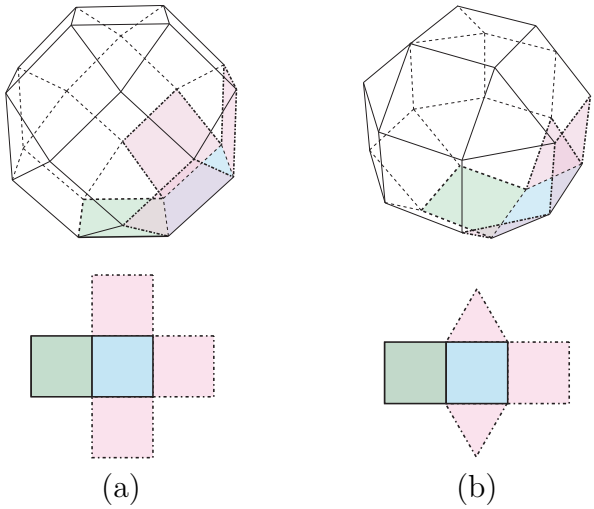

Figure 3.4: Cases of the first three faces in the rotational unfolding for a rhombitruncated cuboctahedron.

Chapter 4

Archimedean and Johnson solids

We implemented rotational unfolding in C++ and adapted it to Archimedean solids and Johnson solids to find their overlapping edge unfoldings [1]. We obtain the following theorems from our experiments.

Theorem 1 (Archimedean solids)**.**

(a) An icosidodecahedron and a rhombitruncated cuboctahedron have no overlapping edge unfoldings.

(b) A snub cube has three types of overlapping unfoldings with two vertices of faces in contact, as shown in Figure 1.3.

Theorem 2 (Johnson solids)**.**

(a) 48 Johnson solids shown in Table 1.2 have no overlapping edge unfoldings.

(b) 44 Johnson solids shown in Table 1.2 have overlapping edge unfoldings, as shown in Appendix A Figure A.1 ∼ A.44.

An overlapping edge unfolding exists for a truncated dodecahedron and a truncated icosahedron [8]. Our algorithm finds the other overlapping unfoldings for truncated icosahedron, as shown in, and we verify that it has no other types of overlapping edge unfoldings. For the 20 Johnson solids, we enumerate overlapping patterns, as shown in Appendix A. We find edge unfoldings with two vertices of faces in contact (Figure A.14, A.15, A.19, A.20, A.21, A.22, A.27, A.28), two edges of faces in contact (Figure A.27, A.28), or a vertex of one face and an edge of the other edge in contact (Figure A.2, A.27, A.28) in Johnson solids.

[1] Johnson Solid image files and adjacency list data were used as published in `https://mitani.cs.tsukuba.ac.jp/polyhedron/data/polyhedron.zip`.

Chapter 5

Archimedean prisms

In this section, we prove Theorem 3.

Theorem 3 (Archimedean prisms)**.** *Let n be a natural number and $P_R(n)$ be an n-gonal Archimedean prism.*

(a) If $3 \leq n \leq 23$, $P_R(n)$ has no overlapping edge unfoldings.

(b) For $n \geq 24$, there exists an overlapping edge unfolding in $P_R(n)$.

We demonstrate the case of no overlapping edge unfolding of Theorem 3 (a) for every $n \in \{3, \ldots, 23\}$ of $P_R(n)$ using rotational unfolding.

Theorem 3 (b) can be proven by constructing an overlapping edge unfolding for $P_R(n)$. Let F_T and F_B be the top and bottom faces of $P_R(n)$, respectively, and $f_0, \cdots, f_{n-1}$ be the sides, which are numbered counterclockwise viewing from the top face F_T. For $i \in \{0, \ldots, n-1\}$, let t_i and b_i be vertices on F_T and F_B such that they share two faces f_i and f_{i+1}, where $f_n = f_0$. For $n = 24$, $P_R(n)$ has an overlapping edge unfolding, as shown in Figure 1.5 (a) (right), consisting of faces $\{F_B, f_0, F_T, f_3, f_2, f_1\}$ obtained by cutting along the thick line of $P_R(n)$, as shown in Figure 1.5 (a) (left). For $25 \leq n \leq 28$, $P_R(n)$ has an overlapping edge unfolding similar to $P_R(24)$, as shown in Figure 5.1.

It remains to be shown that an overlapping edge unfolding of $P_R(n)$ exists for $n \geq 29$. We prove that the edge unfolding consisting of faces $\{F_B, f_0, F_T, f_2, f_1\}$ overlap, as shown in Figure 5.2 (right), by cutting along the thick line of $P_R(n)$ shown in Figure 5.2 (left).

Lemma 3. *For $n \geq 29$, if we cut the edges $(t_0, t_1), (t_0, b_0), (b_0, b_1)$, and (b_1, b_2) and do not cut $(t_{n-1}, t_0), (b_{n-1}, b_0)$, and (t_1, t_2) of $P_R(n)$, any edge unfolding is overlapping.*

Figure 5.3 shows a part of edge unfolding consisting of $\{F_B, f_0, F_T, f_2, f_1\}$, and Figure 5.4 is an enlarged and simplified image of Figure 5.3. We define t_i^T and b_i^B for $i \in \{0, \ldots, n-1\}$ as vertices on F_T and F_B in the edge unfolding such that they are t_i

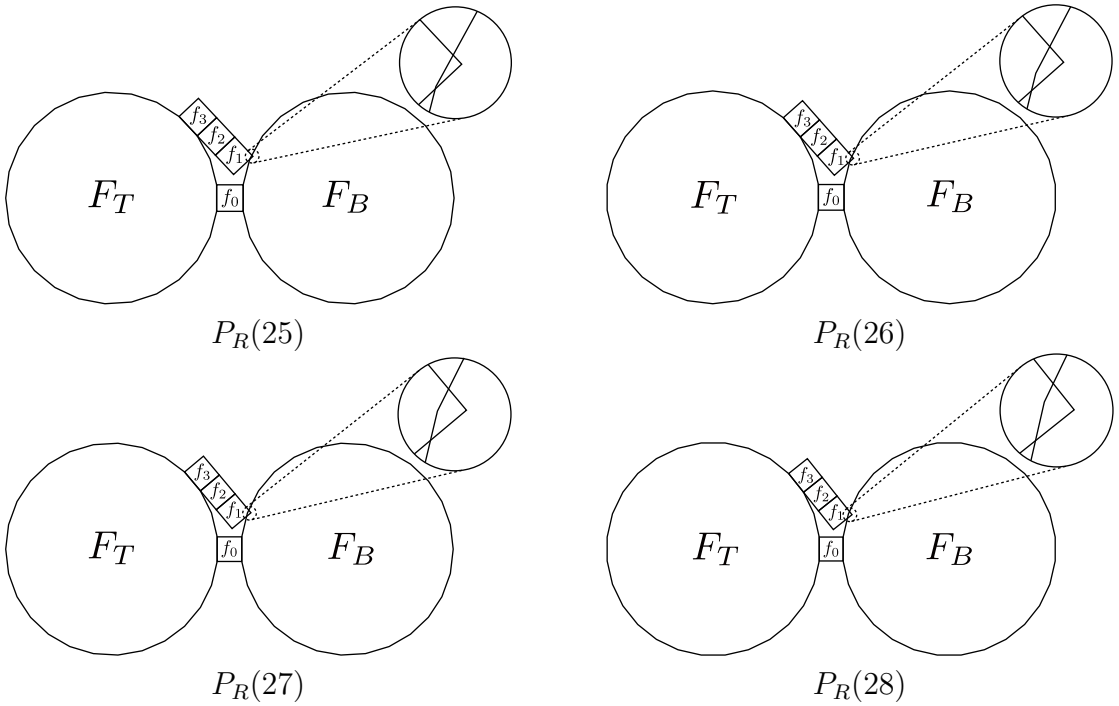

Figure 5.1: Overlapping edge unfoldings of $P_R(25)$ to $P_R(28)$ consisting of faces $\{F_B, f_0, F_T, f_3, f_2, f_1\}$

and b_i in $P_R(n)$, respectively. Let S be a subset of faces $\{f_0, \ldots, f_{n-1}\}$. The vertices t_i and b_i in $P_R(n)$ that are shared by S in the edge unfolding are denoted as t_i^S and b_i^S, respectively. Here, we set $b_0^{f_1}$ and $b_1^{f_1,f_2}$ as $(0,0)$ and $(0,1)$ in the plane, respectively. We can obtain the following lemma.

Lemma 4.

(i) Point b_0^B exists in the third quadrant.

(ii) Point b_1^B exists in the first quadrant.

(iii) Let p_1 be an intersection point of the segment $b_0^B b_1^B$ and the y-axis. The y-coordinate of p_1 is positive.

The y-coordinate of p_1 is within $(0,-1)$ to $(0,1)$ because the length of the line segment $b_0^B b_1^B$ is one if Lemma 4 (i) and (ii) are satisfied. And if the y-coordinate of p_1 is positive, the line segment $b_0^{f_1} b_1^{f_1,f_2}$ intersects the line segment $b_0^B b_1^B$. Therefore, the faces f_1 and F_B overlap if Lemma 4 are satisfied.

We will show that Lemma 4 are satisfied. We define the angle $\theta = \frac{2\pi}{n}$ as the exterior angle of the regular n-sided polygon. The range of θ is $0 < \theta \leq \frac{2\pi}{29}$ because $n \geq 29$. We make the following claim.

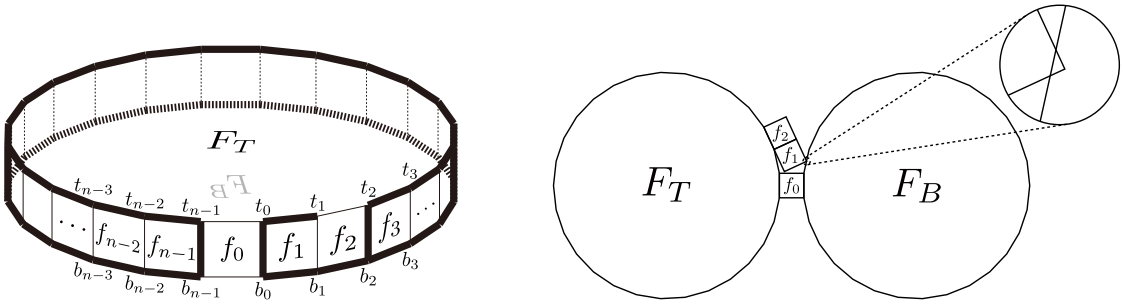

Figure 5.2: An overlapping edge unfolding in the 29-gonal Archimedean prism. The right edge unfolding is obtained by cutting along the thick line of the left convex polyhedron.

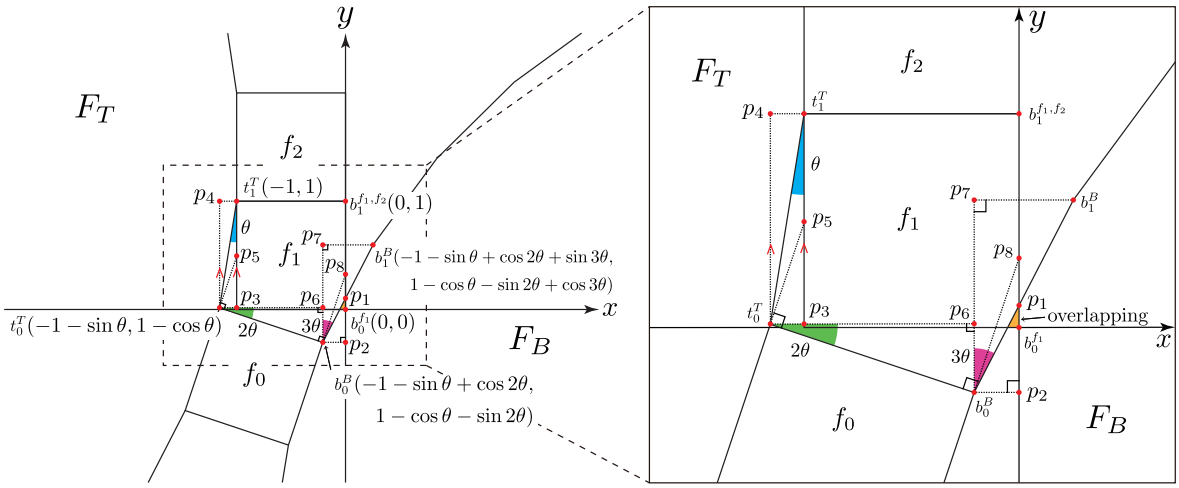

Figure 5.3: Magnified image of overlapping areas in the edge unfolding of $P_R(n)$

Claim 1. *The coordinates of* b_0^B *and* b_1^B *are* $(-1-\sin\theta+\cos 2\theta, 1-\cos\theta-\sin 2\theta)$ *and* $(-1-\sin\theta+\cos 2\theta+\sin 3\theta, 1-\cos\theta-\sin 2\theta+\cos 3\theta)$*, respectively.*

Proof. **(The coordinates of b_0^B)** Let p_3 be the intersection point of the perpendicular line from point t_1^T to the x-axis and the perpendicular line from point t_0^T to the y-axis. The coordinate of point t_0^T is $(-1-\sin\theta, 1-\cos\theta)$ since $\triangle t_1^T p_3 t_0^T$ is a right triangle with an oblique side of length 1. Let p_4 be the intersection point of the auxiliary line drawn parallel to the y-axis with respect to point t_0^T and the auxiliary line extending the line segment $b_1^{f_1,f_2}t_1^T$ in the direction of t_1^T, p_5 be the intersection point of the auxiliary line drawn perpendicular to the line segment $t_0^T b_0^B$ at point t_0^T and the line segment $t_1^T p_3$, and p_6 be the intersection point of the perpendicular line from point b_0^B to the x-axis and the perpendicular line from point t_0^T to the y-axis. $\angle p_4 t_0^T t_1^T$ is θ since $t_0^T p_4 // p_3 t_1^T$, $\angle p_5 t_0^T t_1^T$ is θ since it is the exterior angle of F_T, $\angle p_5 t_0^T p_3$ is $\frac{\pi}{2}-2\theta$ since $\angle p_4 t_0^T p_3$ is a right angle, and $\angle p_6 t_0^T b_0^B$ is 2θ since $\angle p_5 t_0^T b_0^B$ is a right angle. As a result, the coordinate of

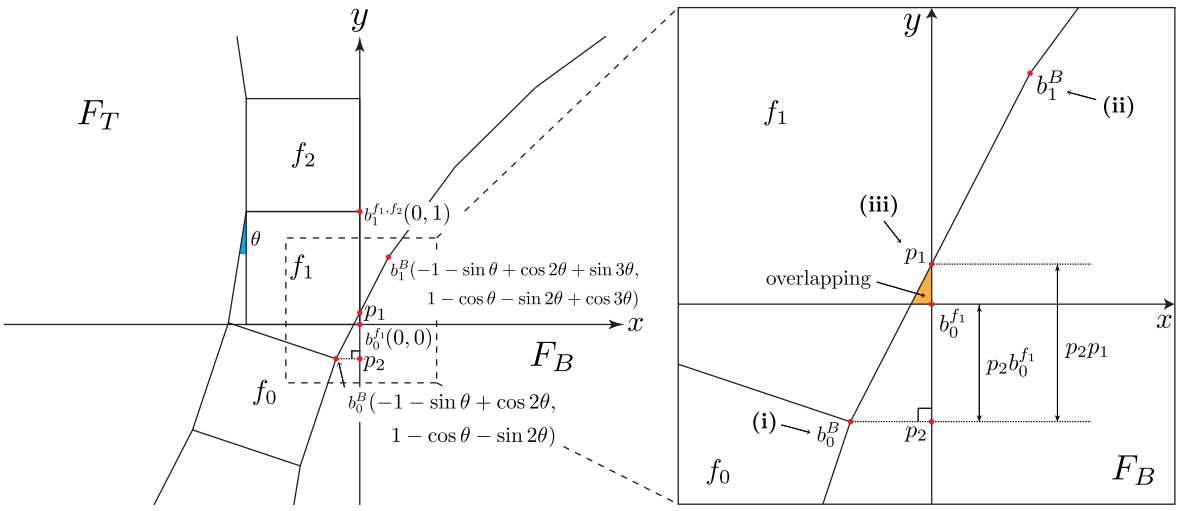

Figure 5.4: Enlarged and simplified image of Figure 5.3

point b_0^B is $(-1-\sin\theta+\cos 2\theta, 1-\cos\theta-\sin 2\theta)$ since $\triangle p_6 t_0^T b_0^B$ is a right triangle with an oblique side of length 1.

(The coordinates of b_1^B) Let p_7 be the intersection point of the perpendicular line from point b_0^B to the x-axis and the perpendicular line from point b_1^B to the y-axis, and p_8 be the intersection point of the auxiliary line drawn perpendicular to the line segment $t_0^T b_0^B$ at point b_0^B and the y-axis. $\angle p_8 b_0^B b_1^B$ is θ since it is the exterior angle of F_T, $\angle p_6 b_0^B t_0^T$ is $\frac{\pi}{2}-2\theta$ since $\triangle b_0^B p_6 t_0^T$ is a right triangle, $\angle p_8 b_0^B p_7 (=\angle p_8 b_0^B p_6)$ is 2θ since $\angle p_8 b_0^B t_0^T$ is a right angle, and $\angle p_7 b_0^B b_1^B$ is 3θ by adding $\angle p_8 b_0^B b_1^B$ and $\angle p_8 b_0^B p_7$. As a result, the coordinate of point b_1^B is $(-1-\sin\theta+\cos 2\theta+\sin 3\theta, 1-\cos\theta-\sin 2\theta+\cos 3\theta)$ since $\triangle b_0^B p_7 b_1^B$ is a right triangle with an oblique side of length 1. □

From Claim 1 and differential analysis, we can show Lemma 4 (i) - (iii).

Proof of Lemma 4. **(i).** For point p, the x and y coordinates are denoted as $x(p)$ and $y(p)$, respectively. For $x(b_0^B)$, we obtain the following inequality since $-\sin\theta < -\sin 0$, $\cos 2\theta < \cos 0$ from the range of θ.

$$x(b_0^B) = -1-\sin\theta+\cos 2\theta < -1-\sin 0+\cos 0 = 0$$

For $y(b_0^B)$, differentiating $y(b_0^B(\theta)) = 1-\cos\theta-\sin 2\theta$, yields:

$$\frac{d}{d\theta}y(b_0^B(\theta)) = -2\cos 2\theta+\sin\theta = 4\left(\sin\theta+\frac{1}{8}\right)^2-\frac{33}{16}$$

Solving $\frac{d}{d\theta}y(b_0^B(\theta)) = 0$ for θ yields the following:

$$\theta = \arcsin\left(\frac{-1\pm\sqrt{33}}{8}\right)+2n\pi \ (n\in\mathbb{N})$$

The definition range for θ is contained between $\arcsin\left(\frac{-1-\sqrt{33}}{8}\right)$ and $\arcsin\left(\frac{-1+\sqrt{33}}{8}\right)$. $y(b_0^B(\theta))$ is a monotonically decreasing function in the definition range of θ since the relation $\arcsin\left(\frac{-1-\sqrt{33}}{8}\right) < 0 < \arcsin\left(\frac{-1+\sqrt{33}}{8}\right)$ holds and $\frac{d}{d\theta}y(b_0^B(0)) = -2$. Hence, the following equation holds since $y(b_0^B(0)) = 0$.

$$y(b_0^B) = 1 - \cos\theta - \sin 2\theta < 0$$

Thus, b_0^B is in the third quadrant.

(ii). For $x(b_1^B)$, differentiating $x(b_1^B(\theta)) = -1 - \sin\theta + \cos 2\theta + \sin 3\theta$, yields:

$$\begin{aligned}\frac{d}{d\theta}x(b_1^B(\theta)) &= \frac{d}{d\theta}(-\sin^2\theta - \cos^2\theta - \sin\theta + \cos^2\theta - \sin^2\theta + 3\sin\theta - 4\sin^3\theta)\\ &= \frac{d}{d\theta}(2\sin\theta - 4\sin^3\theta - 2\sin^2\theta)\\ &= 2\cos\theta(1 - 6\sin^2\theta - 2\sin\theta)\end{aligned}$$

$x(b_1^B(\theta))$ is a monotonically increasing function in the definition range of θ since $-6\sin\theta \geq -6\left(\sin\frac{2\pi}{29}\right)^2$, and $-2\sin\theta \geq -2\sin\frac{2\pi}{29}$. Hence, the following equation holds since $x(b_1^B(0)) = 0$.

$$x(b_1^B) = -1 - \sin\theta + \cos 2\theta + \sin 3\theta > 0$$

For $y(b_1^B)$, we obtain the following inequality since $-\cos\theta > -\cos 0$, $-\sin 2\theta \geq -\sin\frac{4\pi}{29}$, and $\cos 3\theta \geq \cos\frac{6\pi}{29}$ from the range of θ.

$$y(b_1^B) = 1 - \cos\theta - \sin 2\theta + \cos 3\theta > 1 - \cos 0 - \sin\frac{4\pi}{29} + \cos\frac{6\pi}{29} > 0$$

Thus, b_1^B is in the first quadrant.

(iii). Let p_2 be an intersection point of the perpendicular line from point b_0^B to the y-axis and y-axis; that is, the coordinates of p_2 are $(0, 1 - \cos\theta - \sin 2\theta)$. We give the following claim.

Claim 2. *The length of the line segment p_2p_1 is greater than that of $p_2b_0^{f_1}$.*

The length of the line segment $b_0^Bp_2$ is not zero because of the condition **(i)**; therefore, we will show $\frac{p_2b_0^{f_1}}{b_0^Bp_2}$ is larger than $\frac{p_2p_1}{b_0^Bp_2}$.

$\frac{p_2b_0^{f_1}}{b_0^Bp_2}$ and $\frac{p_2p_1}{b_0^Bp_2}$ can be denoted as follows:

$$\frac{p_2b_0^{f_1}}{b_0^Bp_2} = \frac{-1 + \cos\theta + \sin 2\theta}{1 + \sin\theta - \cos 2\theta}, \qquad \frac{p_2p_1}{b_0^Bp_2} = \frac{\cos 3\theta}{\sin 3\theta}$$

Therefore, we can show that the following equation holds.

$$\frac{-1 + \cos\theta + \sin 2\theta}{1 + \sin\theta - \cos 2\theta} < \frac{\cos 3\theta}{\sin 3\theta} \tag{5.1}$$

The definition range of θ is $0 < \theta \leq \frac{2\pi}{29}$; therefore, $1 + \sin\theta - \cos 2\theta > 0$ and $\sin 3\theta > 0$. Multiplying both sides of (5.1) by $(1 + \sin\theta - \cos 2\theta)\sin 3\theta$ and expanding, resulting in the following equation is obtained.

$$-\sin 3\theta + \sin 3\theta\cos\theta + \sin 3\theta\sin 2\theta - \cos 3\theta - \cos 3\theta\sin\theta + \cos 3\theta\cos 2\theta < 0$$

Let $f(\theta) = -\sin 3\theta - \cos 3\theta + \sin 2\theta + \cos\theta$. The derivative of $f(\theta)$, yields:

$$\begin{aligned} f'(\theta) &= -3\cos 3\theta + 3\sin 3\theta + 2\cos 2\theta - \sin\theta \\ &= (\sin\theta + \cos\theta)(6\sin 2\theta + 2\cos\theta - 2\sin\theta - 3) - \sin\theta \end{aligned}$$

Let $f'(\theta) = g(\theta) - \sin\theta$. Differentiating $g(\theta)$, gives:

$$\begin{aligned} g'(\theta) &= 12\cos 2\theta - 2\sin\theta - 2\cos\theta \\ &= 2(\sin\theta + \cos\theta)\left(6\sin\left(\theta + 3\pi/4\right) - 1\right) > 0 \end{aligned}$$

Hence, $g(\theta)$ is a monotonically increasing function that switches from negative to positive midway since $g(0) < 0$ and $g\left(\frac{2\pi}{29}\right) > 0$. Rigorous numerical calculations show a negative to positive transition between $n = 62$ and $n = 63$. Therefore, for $n \geq 62$, $f(\theta) < 0$ since $f(\theta)$ is a monotonically decreasing function and $f(0) = 0$. By contrast, for $29 \leq n \leq 61$, $f(\theta) < 0$ from the numerical calculation of $\frac{p_2 b_0^{f_1}}{b_0^B p_2}$ and $\frac{p_2 p_1}{b_0^B p_2}$. Thus, the length of the line segment $p_2 p_1$ is greater than that of $p_2 b_0^{f_1}$. □

Thus, Lemma 4 (i) - (iii) hold; that is, an overlapping edge unfolding exists for $P_R(n)$, where $n \geq 29$.

Chapter 6

Archimedean anti-prisms

In this section, we prove Theorem 4.

Theorem 4 (Archimedean anti-prisms)**.** *Let n be a natural number and $P_A(n)$ be an n-gonal Archimedean antiprism.*

(a) If $3 \leq n \leq 11$, $P_A(n)$ has no overlapping edge unfoldings.

(b) For $n \geq 12$, there exists an overlapping edge unfolding in $P_A(n)$.

We demonstrate the no overlapping edge unfolding of Theorem 4 (a) for every $n \in \{3, \ldots, 11\}$ of $P_A(n)$ using rotational unfolding.

Theorem 4 (b) can be proven by constructing an overlapping edge unfolding for $P_A(n)$. Let F_T and F_B be the top and bottom faces of $P_A(n)$, respectively, and $f_0, \cdots, f_{2n-1}$ be the sides, which are numbered counterclockwise viewing from the top face F_T. For $i \in \{0, \ldots, n-1\}$, let t_i and b_i be vertices on F_T and F_B such that they share three faces f_{2i}, f_{2i+1}, and f_{2i+2} and f_{2i-1}, f_{2i}, and f_{2i+1}, where $f_{-1} = f_{2n-1}$ and $f_{2n} = f_0$. For $n = 12$, $P_A(n)$ has an overlapping edge unfolding, as shown in Figure 1.5 (b) (right), consisting of faces $\{f_3, F_B, f_5, f_4, F_T, f_0, f_1, f_2\}$ obtained by cutting along the thick line of $P_A(n)$, as shown in Figure 1.5 (b) (left). For $13 \leq n \leq 16$, $P_A(n)$ has an overlapping edge unfolding similar to $P_A(12)$, as shown in Figure 6.1. For $n \in \{17, 18\}$, $P_A(n)$ has overlapping edge unfoldings consisting of faces $\{F_T, f_0, f_1, F_B, f_5, f_4, f_3, f_2\}$, as shown in Figure 6.2 (left), obtained by cutting along the thick line $P_A(n)$, as shown in Figure 6.2 (right).

It remains to be shown that an overlapping edge unfolding of $P_A(n)$ exists for $n \geq 19$. We can prove that the edge unfolding consisting of faces $\{F_B, f_1, f_2, F_T, f_4, f_3\}$ contains overlapping, as shown in Figure 6.3 (right), by cutting along the thick line of $P_A(n)$, as shown in Figure 6.3 (left).

Lemma 5. *For $n \geq 19$, if we cut the edges (t_1, b_1) and (b_1, b_2) and do not cut the edges $(b_0, b_1), (t_0, t_1), (t_0, b_1), (t_1, t_2)$, and (t_1, b_2) of $P_A(n)$, any edge unfolding is overlapping.*

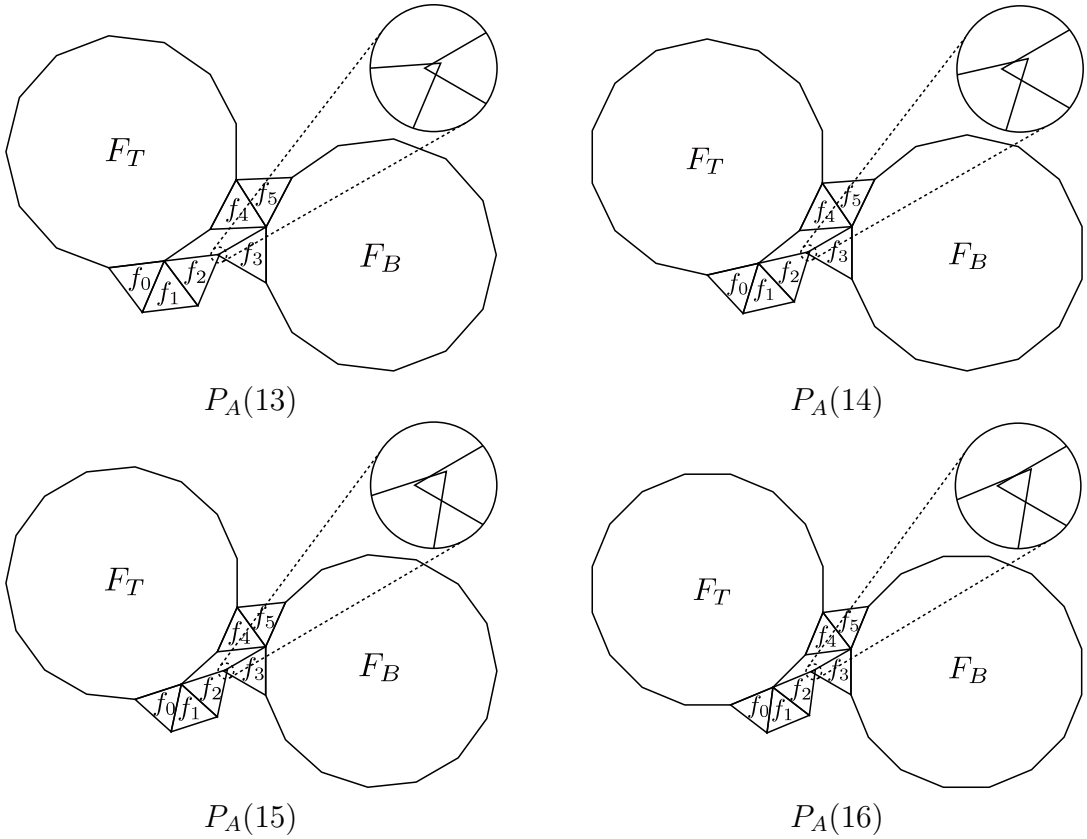

Figure 6.1: Overlapping edge unfoldings of $P_A(13)$ to $P_A(16)$ consisting of faces $\{f_3, F_B, f_5, f_4, F_T, f_0, f_1, f_2\}$

Figure 6.4 shows a part of edge unfolding consisting of $\{F_B, f_1, f_2, F_T, f_4, f_3\}$, and Figure 6.5 is an enlarged and simplified image of Figure 6.4. We define t_i^T and b_i^B for $i \in \{0 \cdots n-1\}$ as vertices on F_T and F_B in the edge unfolding such that they are t_i and b_i in $P_A(n)$, respectively. Let S be a subset of faces $\{f_0, \ldots, f_{2n-1}\}$. The vertices t_i and b_i are vertices in $P_A(n)$ that are shared by S in the edge unfolding are denoted as t_i^S and b_i^S, respectively. Here, we set $b_1^{f_3}$ and t_1^T as $(0,0)$ and $(-1,0)$ in the plane, respectively. We can obtain the following lemma.

Lemma 6.

(i) Point b_1^B exists in the third quadrant.

(ii) The y-coordinate of point b_2^B is positive.

(iii) Let p_1 be an intersection point of the segment $b_1^B b_2^B$ and the x-axis. The x-coordinate of point p_1 is in $-1 < p_1 < 0$.

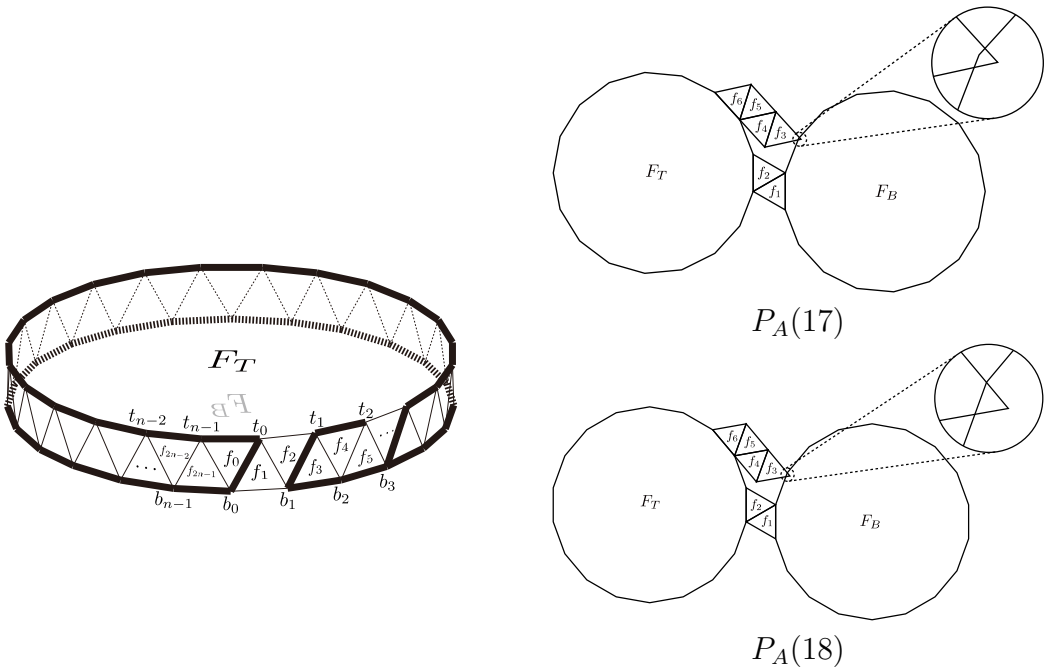

Figure 6.2: Overlapping edge unfoldings of $P_A(17)$ and $P_A(18)$, consisting of the set of faces $\{F_T, f_0, f_1, F_B, f_5, f_4, f_3, f_2\}$. The right edge unfolding are obtained by cutting along the thick line of the left convex polyhedron.

Face f_3 is a triangle such that the bottom is $(-1, 0)$ to $(0, 0)$. From Lemma 6 (i) and (ii), there exists an intersection point p_1 of the segment the segment $b_1^B b_2^B$ and the x-axis. Moreover, if p_1 is within $(-1, 0)$ to $(0, 0)$, the line segment $b_1^B b_2^B$ intersects f_3; that is, f_3 and F_B overlap.

We define the angle $\theta = \frac{2\pi}{n}$ as the exterior angle of the regular n-sided polygon. The range of θ is $0 < \theta \leq \frac{2\pi}{19}$ because $n \geq 19$. We obtain the following claim.

Claim 3. *The coordinate of b_1^B is $(-1 + \cos\theta, -\sin\theta)$, the coordinate of b_2^B is*

$$\begin{cases} \left(-1 + \cos\theta + \sin\left(2\theta - \frac{\pi}{6}\right), -\sin\theta + \cos\left(2\theta - \frac{\pi}{6}\right)\right) & \text{if } 19 \leq n \leq 24 \\ \left(-1 + \cos\theta - \sin\left(\frac{\pi}{6} - 2\theta\right), -\sin\theta + \cos\left(\frac{\pi}{6} - 2\theta\right)\right) & \text{if } n \geq 25 \end{cases}$$

and the x-coordinate of p_1 is

$$\begin{cases} \cos\left(\frac{\pi}{6} - \theta\right) / \cos\left(2\theta - \frac{\pi}{6}\right) - 1 & \text{if } 19 \leq n \leq 24 \\ \cos\left(\frac{\pi}{6} - \theta\right) / \cos\left(\frac{\pi}{6} - 2\theta\right) - 1 & \text{if } n \geq 25. \end{cases}$$

Proof. **(The coordinates of b_1^B)** Let p_2 be the intersection point of the perpendicular line from point b_1^B to the x-axis and x-axis, and p_3 be the intersection point of the auxiliary line extending the line segment $t_2^T t_1^T$ in the t_1^T direction and the line segment

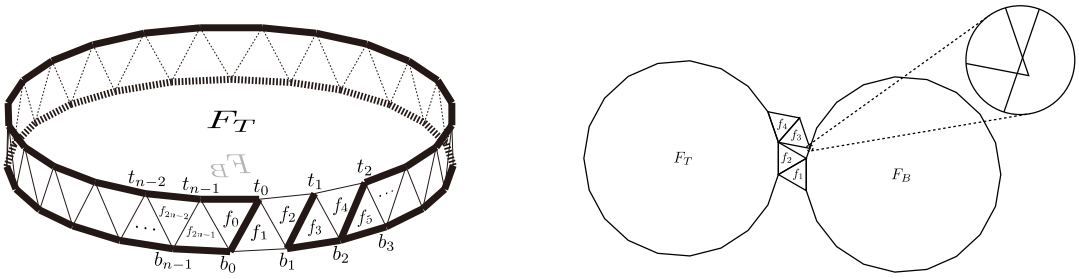

Figure 6.3: An overlapping edge unfolding in the 19-gonal Archimedean prism. We obtain the right edge unfolding by cutting along the thick line of the left convex polyhedron.

$t_0^T b_1^B$. $\angle p_3 t_1^T b_1^B$ is $\frac{\pi}{3} - \theta$ since $\angle t_0^T t_1^T b_1^B$ is $\frac{\pi}{3}$, and the $\angle p_2 t_1^T b_1^B$ is θ since $\angle p_3 t_1^T p_2$ is $\frac{\pi}{3}$. As a result, the coordinate of point b_1^B is $(-1 + \cos\theta, -\sin\theta)$ since $\triangle t_1^T p_2 b_1^B$ is a right triangle with an oblique side of length 1.

(The coordinates of b_2^B) The coordinates of point b_2^B are divided into two cases concerning the value of n. Let p_4 be the intersection point of the perpendicular line from point b_2^B to the y-axis and the perpendicular line from point b_1^B to the x-axis, p_5 be the intersection point of the auxiliary line extending the line segment $b_2^B b_1^B$ in the b_1^B direction and the line segment $t_0^T b_0^B$, and p_6 be the intersection point of the auxiliary line extending the line segment $b_0^B b_1^B$ in the b_1^B direction and the x-axis.

(For $19 \leq n \leq 24$) $\angle t_0^T b_1^B p_5$ is $\frac{\pi}{3} - \theta$ since $\angle b_0^B b_1^B t_0^T$ is the exterior angle of F_B, $\angle p_2 b_1^B t_1^T$ is $\frac{\pi}{2} - \theta$ since $\triangle t_1^T p_2 b_1^B$ is a right triangle, and $\angle b_2^B b_1^B p_4$ is $2\theta - \frac{\pi}{6}$ by subtracting $\angle p_5 b_1^B b_2^B = \pi$ from $(\angle t_0^T b_1^B p_5 + \angle t_1^T b_1^B t_0^T + \angle p_2 b_1^B t_1^T = (\frac{\pi}{3} - \theta) + \frac{\pi}{3} + (\frac{\pi}{2} - \theta) = \frac{7\pi}{6} - 2\theta)$. As a result, the coordinate of point b_2^B is $\left(-1 + \cos\theta + \sin\left(2\theta - \frac{\pi}{6}\right), -\sin\theta + \cos\left(2\theta - \frac{\pi}{6}\right)\right)$ since $\triangle b_2^B p_4 b_1^B$ is a right triangle with an oblique side of length 1.

(For $n \geq 25$) $\angle t_1^T b_1^B b_2^B$ is $\frac{\pi}{3} + \theta$ by adding $\angle t_1^T b_1^B p_6 = \frac{\pi}{3}$ and $\angle p_6 b_1^B p_2 = \theta$, and $\angle b_2^B b_1^B p_4$ is $\frac{\pi}{6} - 2\theta$ by subtracting $\angle p_2 b_1^B t_1^T$ from $\angle t_1^T b_1^B b_2^B$. As a result, the coordinate of point b_2^B is $\left(-1 + \cos\theta - \sin\left(\frac{\pi}{6} - 2\theta\right), -\sin\theta + \cos\left(\frac{\pi}{6} - 2\theta\right)\right)$ since $\triangle b_2^B p_4 b_1^B$ is a right triangle with an oblique side of length 1.

(The coordinates of p_1) The equation of the line with points b_1^B and b_2^B yields:

$$y(\theta) = \frac{y(b_2^B) - y(b_1^B)}{x(b_2^B) - x(b_1^B)}(x - x(b_1^B)) + y(b_1^B) = \frac{\cos\left(\angle b_2^B b_1^B p_4\right)}{\sin\left(\angle b_2^B b_1^B p_4\right)}(x + 1 - \cos\theta) - \sin\theta$$

For point p, the x and y coordinates are denoted as $x(p)$ and $y(p)$, respectively. $x(p_1)$ yields the following since $y(p_1) = 0$.

$$x(p_1) = \frac{\cos\theta\cos\left(\angle b_2^B b_1^B p_4\right) + \sin\theta\sin\left(\angle b_2^B b_1^B p_4\right)}{\cos\left(\angle b_2^B b_1^B p_4\right)} - 1$$

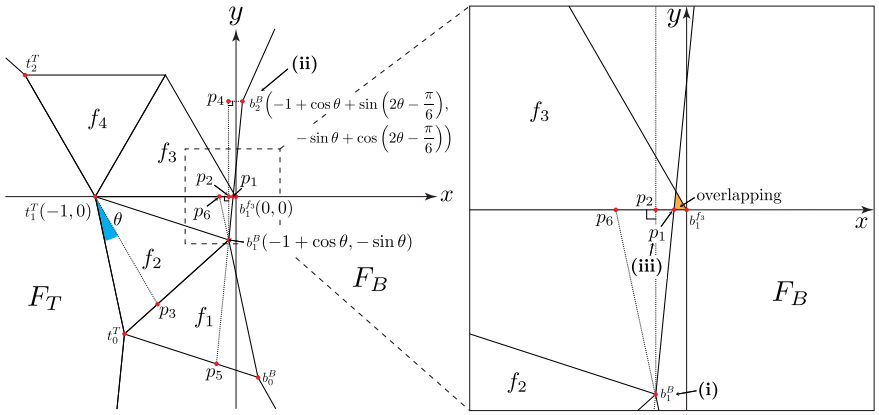

(a) The case for $19 \leq n \leq 24$

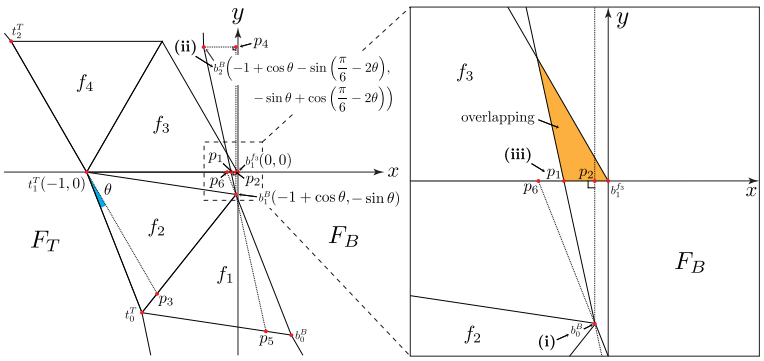

(b) The case for $n \geq 25$

Figure 6.4: Magnified image of overlapping areas in the edge unfolding of $P_A(n)$

As a result, the x-coordinate of p_1 is $\begin{cases} \frac{\cos\left(\frac{\pi}{6}-\theta\right)}{\cos\left(2\theta-\frac{\pi}{6}\right)}-1 & \text{if } 19 \leq n \leq 24 \\ \frac{\cos\left(\frac{\pi}{6}-\theta\right)}{\cos\left(\frac{\pi}{6}-2\theta\right)}-1 & \text{if } n \geq 25 \end{cases}$ □

From Claim 3 and differential analysis, we can show Lemma 6 (i) - (iii).

Proof of Lemma 6. **(i).** For $x(b_1^B)$, we obtain the following inequality since $\cos\theta < \cos 0$.

$$b_{1x}^B = -1 + \cos\theta < -1 + \cos 0 = 0$$

For $y(b_1^B)$, we obtain the following inequality since $-\sin\theta < -\sin\theta$.

$$b_{1y}^B = -\sin\theta < -\sin 0 = 0$$

Thus, b_1^B is in the third quadrant.

(ii). (For $19 \leq n \leq 24$**)** For $y(b_2^B)$, we obtain the following inequality since $-\sin\theta \geq -\sin\frac{2\pi}{19}$, $\cos 2\theta \geq \cos\frac{4\pi}{19}$, and $\sin 2\theta \geq \sin\frac{4\pi}{24}$.

$$\begin{aligned} y(b_2^B) &= -\sin\theta + \cos\left(2\theta - \frac{\pi}{6}\right) = -\sin\theta + \cos 2\theta\cos\frac{\pi}{6} + \sin 2\theta\sin\frac{\pi}{6} \\ &\geq -\sin\frac{2\pi}{19} + \frac{\sqrt{3}}{2}\cos\frac{4\pi}{19} + \frac{1}{2}\sin\frac{4\pi}{24} > 0 \end{aligned}$$

Thus, $y(b_2^B)$ is positive.

(For $n \geq 25$**)** For $y(b_2^B)$, we obtain the following inequality since $-\sin\theta \geq -\sin\frac{2\pi}{25}$, $\cos 2\theta \geq \cos\frac{4\pi}{25}$, $\sin 2\theta > \sin 0$.

$$\begin{aligned} y(b_2^B) &= -\sin\theta + \cos\left(\frac{\pi}{6} - 2\theta\right) = -\sin\theta + \cos\frac{\pi}{6}\cos 2\theta + \sin\frac{\pi}{6}\sin 2\theta \\ &> -\sin\frac{2\pi}{25} + \frac{\sqrt{3}}{2}\cos\frac{4\pi}{25} > 0 \end{aligned}$$

Thus, $y(b_2^B)$ is positive.

(iii). (For $19 \leq n \leq 24$**)** First, we prove $x(p_1) > -1$, that is, $\frac{\cos\left(\frac{\pi}{6}-\theta\right)}{\cos\left(2\theta-\frac{\pi}{6}\right)} > 0$. For $\frac{\pi}{12} \leq \theta \leq \frac{2\pi}{19}$, we obtain the following:

- $\cos\left(\frac{\pi}{6} - \theta\right)$ is a monotonically increasing function, and $\cos\left(\frac{\pi}{6} - \frac{\pi}{12}\right) > 0$.
- $\cos\left(2\theta - \frac{\pi}{6}\right)$ is monotonically decreasing function, and $\cos\left(2 \times \frac{2\pi}{19} - \frac{\pi}{6}\right) > 0$.

As a result, $\cos\left(\frac{\pi}{6} - \theta\right) > 0$ and $\cos\left(2\theta - \frac{\pi}{6}\right) > 0$, that is, $\frac{\cos\left(\frac{\pi}{6}-\theta\right)}{\cos\left(2\theta-\frac{\pi}{6}\right)} > 0$. Thus, $x(p_1) > -1$.

Next, we prove $x(p_1) < 0$, that is, $\frac{\cos\left(\frac{\pi}{6}-\theta\right)}{\cos\left(2\theta-\frac{\pi}{6}\right)} < 1$. For $\frac{\pi}{12} \leq \theta \leq \frac{2\pi}{19}$, we obtain the following:

- $\cos\left(\frac{\pi}{6} - \theta\right)$ is a monotonically increasing function, and $\cos\left(2\theta - \frac{\pi}{6}\right)$ is a monotonically decreasing function.
- $\cos\left(2 \times \frac{\pi}{12} - \frac{\pi}{6}\right) > \cos\left(\frac{\pi}{6} - \frac{\pi}{12}\right)$ and $\cos\left(2 \times \frac{2\pi}{19} - \frac{\pi}{6}\right) > \cos\left(\frac{\pi}{6} - \frac{2\pi}{19}\right)$

As a result, $\cos\left(2\theta - \frac{\pi}{6}\right)$ is larger than $\cos\left(\frac{\pi}{6} - \theta\right)$, that is $\frac{\cos\left(\frac{\pi}{6}-\theta\right)}{\cos\left(2\theta-\frac{\pi}{6}\right)} < 1$. Thus, we have $x(p_1) < 0$.

(For $n \geq 25$**)** First, we prove $x(p_1) > -1$, that is, $\frac{\cos\left(\frac{\pi}{6}-\theta\right)}{\cos\left(\frac{\pi}{6}-2\theta\right)} > 0$. For $0 < \theta \leq \frac{2\pi}{25}$, we obtain the following:

- $\cos\left(\frac{\pi}{6} - \theta\right)$ is a monotonically increasing function, and $\cos\left(\frac{\pi}{6}\right) > 0$.
- $\cos\left(\frac{\pi}{6} - 2\theta\right)$ is a monotonically increasing function and $\cos\left(\frac{\pi}{6}\right) > 0$

Thus, $\cos\left(\frac{\pi}{6}-\theta\right) > 0$ and $\cos\left(\frac{\pi}{6}-2\theta\right) > 0$, that is, $x(p_1) > -1$.

Next, we prove $x(p_1) < 0$, that is, $\frac{\cos\left(\frac{\pi}{6}-\theta\right)}{\cos\left(\frac{\pi}{6}-2\theta\right)} < 1$. For $0 < \theta \leq \frac{2\pi}{25}$, we obtain the following:

- $\cos\left(\frac{\pi}{6}-\theta\right)$ is a monotonically increasing function, and $\cos\left(\frac{\pi}{6}-2\theta\right)$ is a monotonically increasing function.
- $\cos\left(2\times 0-\frac{\pi}{6}\right) = \cos\left(0-\frac{\pi}{6}\right)$ and $\cos\left(2\times\frac{2\pi}{25}-\frac{\pi}{6}\right) > \cos\left(\frac{2\pi}{25}-\frac{\pi}{6}\right)$

As a result, $\cos\left(\frac{\pi}{6}-2\theta\right)$ is larger than $\cos\left(\frac{\pi}{6}-\theta\right)$, that is $\frac{\cos\left(\frac{\pi}{6}-\theta\right)}{\cos\left(\frac{\pi}{6}-2\theta\right)} < 1$. Thus, we have $x(p_1) < 0$. □

Thus, Lemma 6 (i) - (iii) hold; that is, an overlapping edge unfolding exists for $P_A(n)$, where $n \geq 19$.

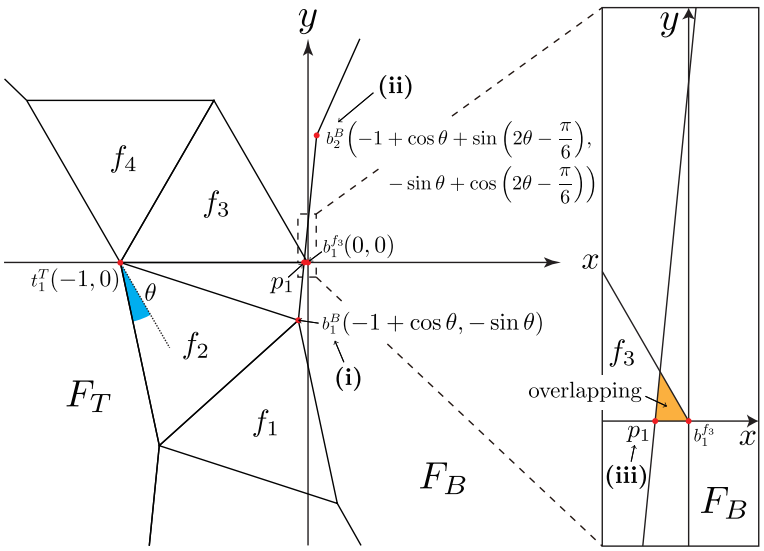

(a) The case for $19 \leq n \leq 24$

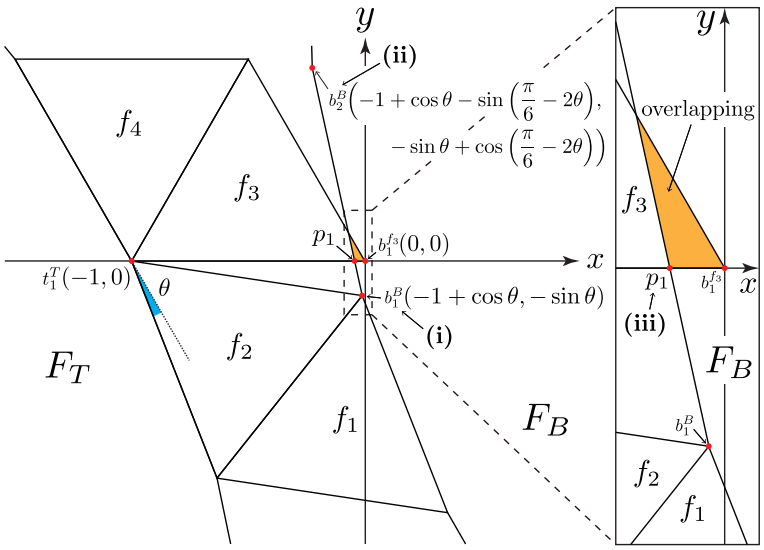

(b) The case for $n \geq 25$

Figure 6.5: Enlarged and simplified image of Figure 6.4

References

[1] Therese C. Biedl, Erik D. Demaine, Martin L. Demaine, Anna Lubiw, Mark H. Overmars, Joseph O'Rourke, Steve Robbins, and Sue Whitesides. Unfolding some classes of orthogonal polyhedra. In *10th Canadian Conference on Computational Geometry*, 1998.

[2] Hallard T. Croft, Kenneth J. Falconer, and Richard K. Guy. *Unsolved Problems in Geometry*. Springer-Verlag, reissue edition, 1991.

[3] Albrecht Dürer. Underweysung der messung, mit dem zirckel und richtscheyt in linien ebenen unnd gantzen corporen, 1525.

[4] Erik D. Demaine and Joseph O'Rourke. *Geometric Folding Algorithms: Linkages, Origami, Polyhedra*. Cambridge University Press, 2007.

[5] Kristin DeSplinter, Satyan L. Devadoss, Jordan Readyhough, and Bryce Wimberly. Nets of higher-dimensional cubes. In *32nd Canadian Conference on Computational Geometry*, 2020.

[6] Branko Grünbaum. Are your polyhedra the same as my polyhedra? In *Discrete and Computational Geometry*, volume 25, pages 461–488. Springer, 2003.

[7] Kenta Hirose. Hanseitamentai no tenkaizu no kasanari ni tsuite (On the overlap of Archimedean solids), in Japanese, 2015. Saitama Univ. graduation thesis. Supervisor : Takashi Horiyama.

[8] Takashi Horiyama and Wataru Shoji. Edge unfoldings of platonic solids never overlap. In *23rd Canadian Conference on Computational Geometry*, 2011.

[9] Takashi Horiyama and Wataru Shoji. The number of different unfoldings of polyhedra. In *24th International Symposium on Algorithms and Computation*, volume 8283 of *LNCS*, pages 623–633. Springer, 2013.

[10] Norman Johnson. Convex polyhedra with regular faces. *Canadian Journal of Mathematics*, 18:169–200, 01 1966.

[11] David M. Mount. On finding shortest paths on convex polyhedra. Technical report, Center for Automation Research, University of Maryland College Park, 1985.

[12] Makoto Namiki and Komei Fukuda. Unfolding 3-dimensional convex polytopes. *A package for Mathematica 1.2 or 2.0. Mathematica Notebook*, 1993.

[13] Wolfram Schlickenrieder. *Nets of Polyhedra*. PhD thesis, Berlin: Technische Universität Berlin, 1997.

[14] Micha Sharir and Amir Schorr. On shortest paths in polyhedral spaces. *SIAM J. Comput.*, 15(1):193–215, 1986.

Appendix A

Reference drawings

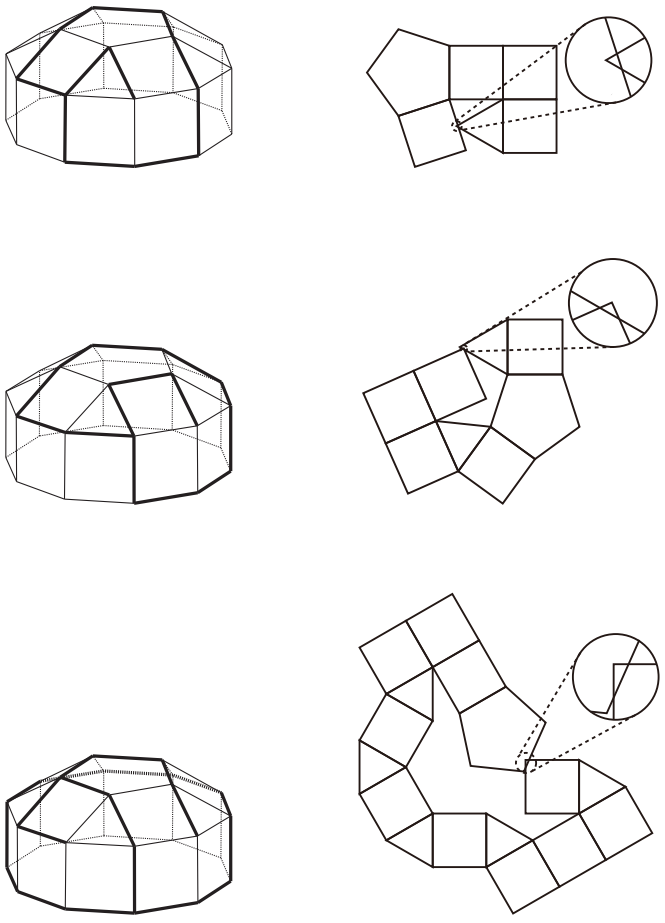

Figure A.1: Overlapping edge unfoldings in an elongated pentagonal cupola (J20). The right edge unfoldings are obtained by cutting along the thick line of the left convex polyhedrons. It has no other types of overlapping edge unfoldings.

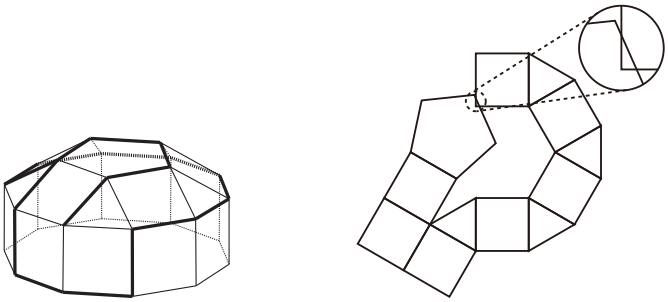

Figure A.1: Overlapping edge unfoldings in an elongated pentagonal cupola (J20). The right edge unfoldings are obtained by cutting along the thick line of the left convex polyhedrons. It has no other types of overlapping edge unfoldings. (continue)

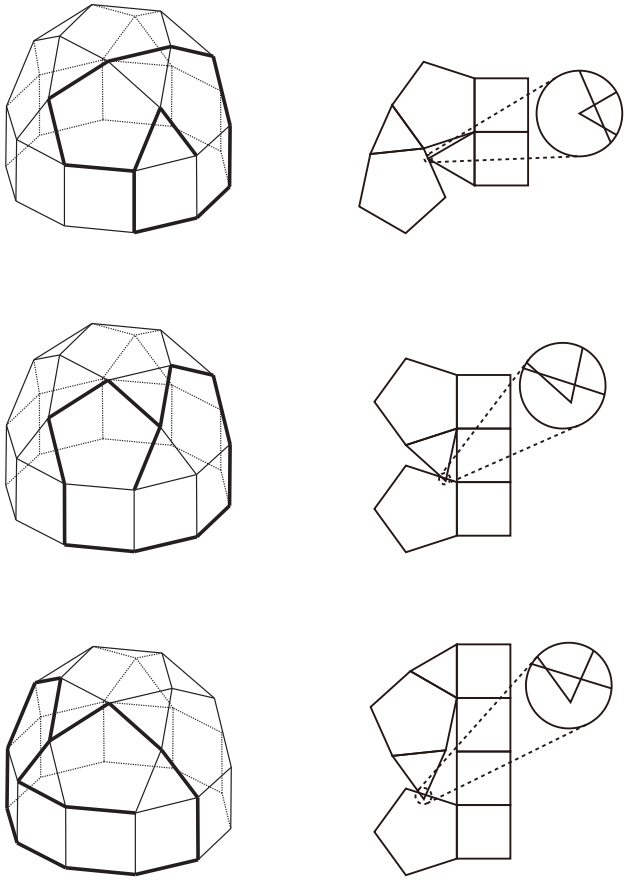

Figure A.2: Overlapping edge unfoldings in an elongated pentagonal rotunda (J21). The right edge unfoldings are obtained by cutting along the thick line of the left convex polyhedrons. It has no other types of overlapping edge unfoldings.

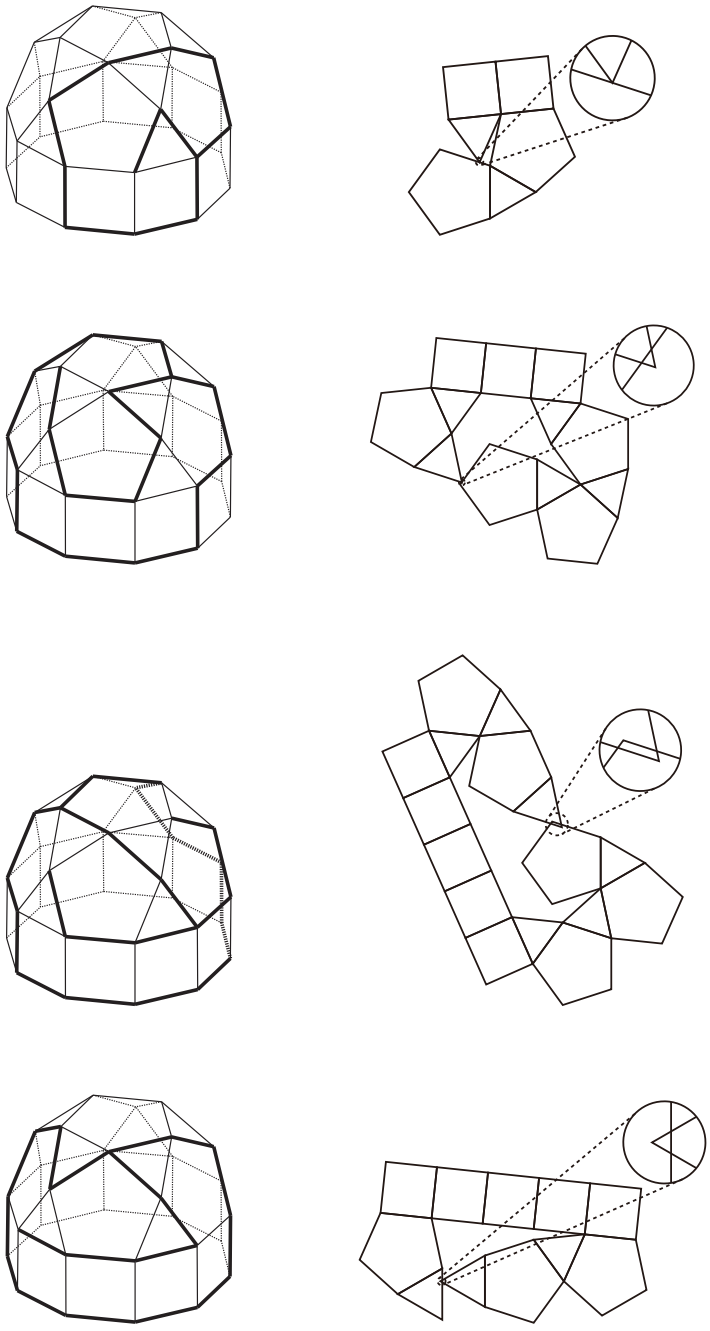

Figure A.2: Overlapping edge unfoldings in an elongated pentagonal rotunda (J21). The right edge unfoldings are obtained by cutting along the thick line of the left convex polyhedrons. It has no other types of overlapping edge unfoldings. (continue)

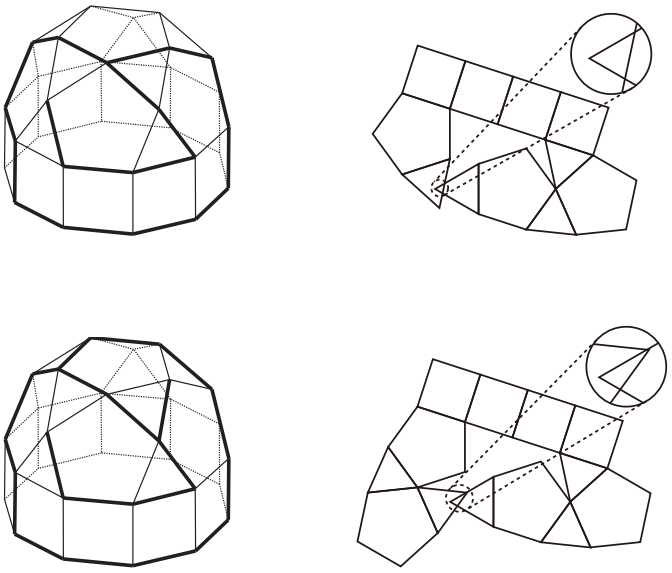

Figure A.2: Overlapping edge unfoldings in an elongated pentagonal rotunda (J21). The right edge unfoldings are obtained by cutting along the thick line of the left convex polyhedrons. It has no other types of overlapping edge unfoldings. (continue)

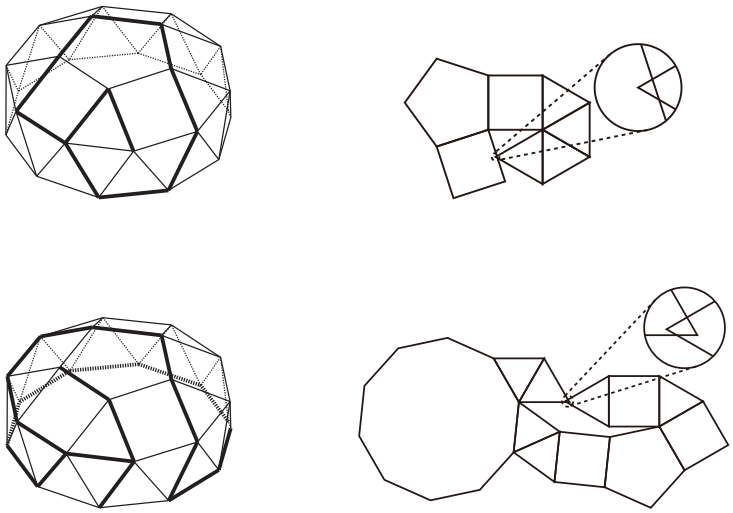

Figure A.3: Overlapping edge unfoldings in a gyroelongated pentagonal cupola (J24). The right edge unfoldings are obtained by cutting along the thick line of the left convex polyhedrons. It has no other types of overlapping edge unfoldings.

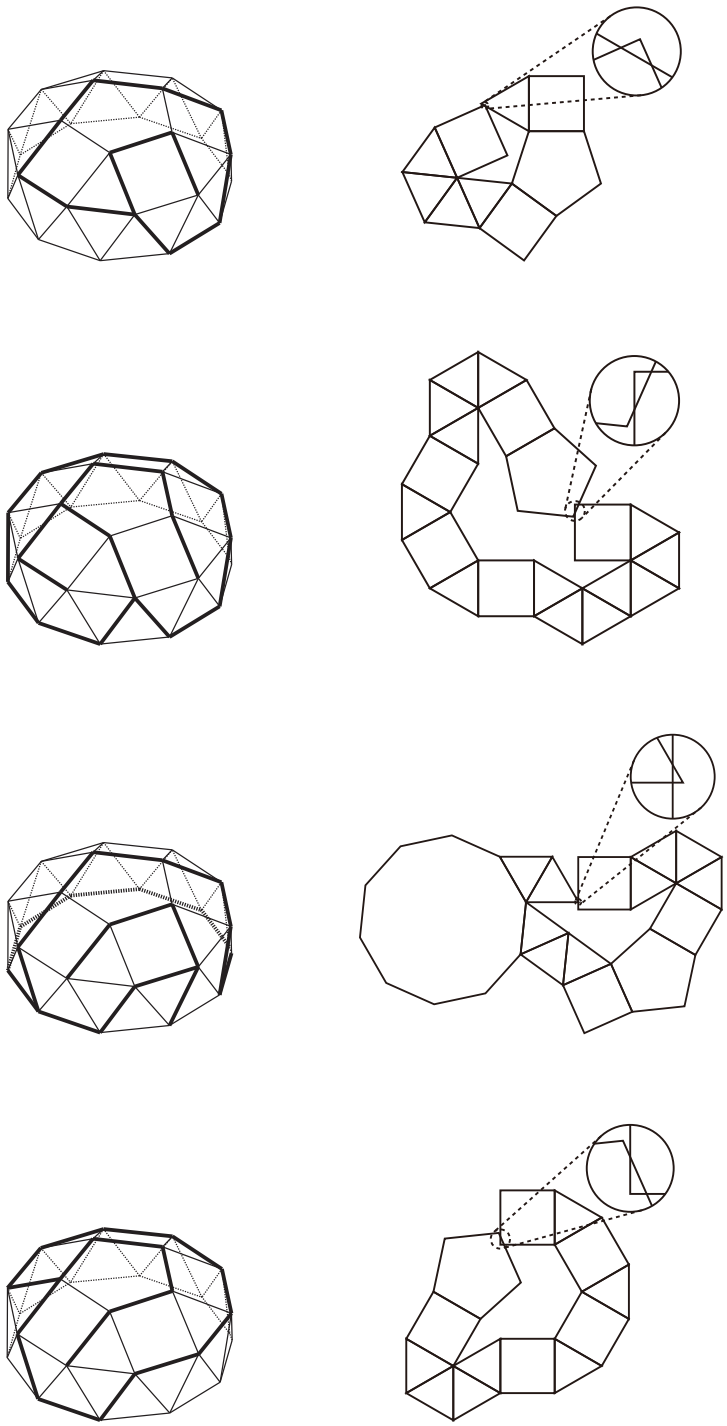

Figure A.3: Overlapping edge unfoldings in a gyroelongated pentagonal cupola (J24). The right edge unfoldings are obtained by cutting along the thick line of the left convex polyhedrons. It has no other types of overlapping edge unfoldings. (continue)

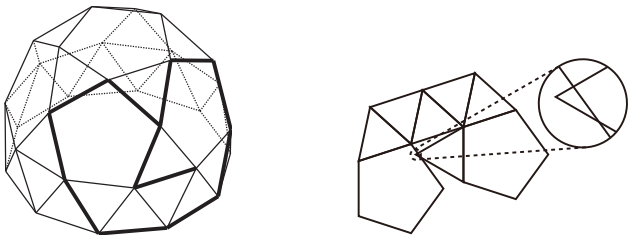

Figure A.4: An overlapping edge unfolding in a gyroelongated pentagonal rotunda (J25). The right edge unfoldings are obtained by cutting along the thick line of the left convex polyhedrons.

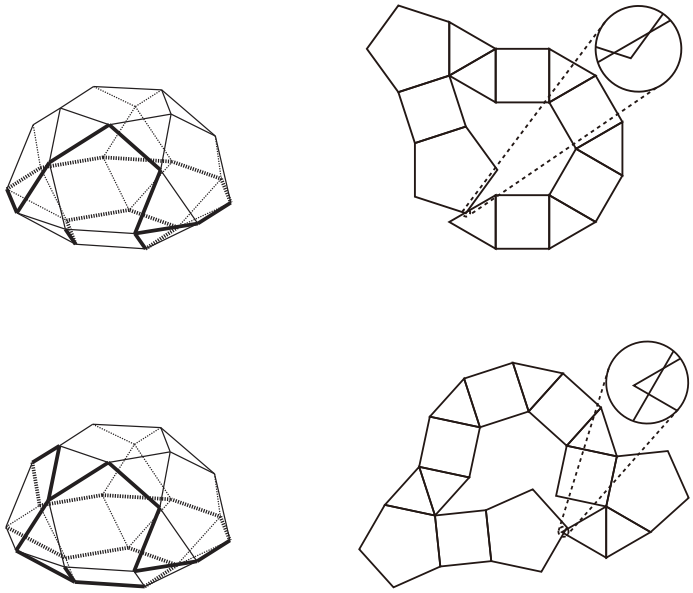

Figure A.5: Overlapping edge unfoldings in a pentagonal orthocupolarotunda (J32). The right edge unfoldings are obtained by cutting along the thick line of the left convex polyhedrons. It has no other types of overlapping edge unfoldings.

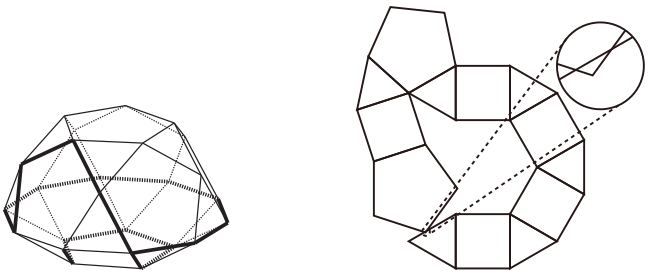

Figure A.6: Overlapping edge unfoldings in a pentagonal gyrocupolarotunda (J33). The right edge unfoldings are obtained by cutting along the thick line of the left convex polyhedrons. It has no other types of overlapping edge unfoldings.

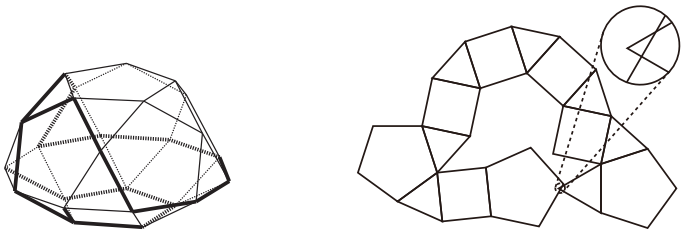

Figure A.6: Overlapping edge unfoldings in a pentagonal gyrocupolarotunda (J33). The right edge unfoldings are obtained by cutting along the thick line of the left convex polyhedrons. It has no other types of overlapping edge unfoldings. (continue)

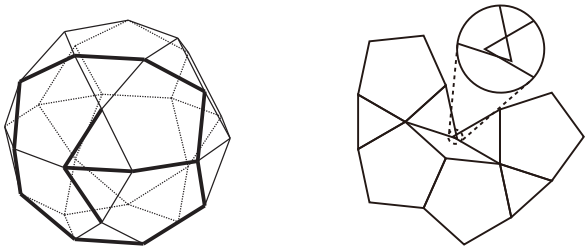

Figure A.7: Overlapping edge unfoldings in a pentagonal orthobirotunda (J34). The right edge unfoldings are obtained by cutting along the thick line of the left convex polyhedrons. It has no other types of overlapping edge unfoldings.

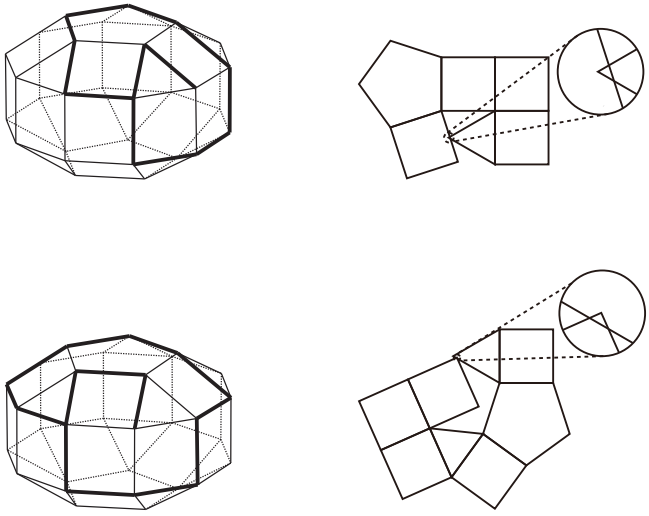

Figure A.8: Overlapping edge unfoldings in an elongated pentagonal gyrobicupola (J38). The right edge unfoldings are obtained by cutting along the thick line of the left convex polyhedrons. It has no other types of overlapping edge unfoldings.

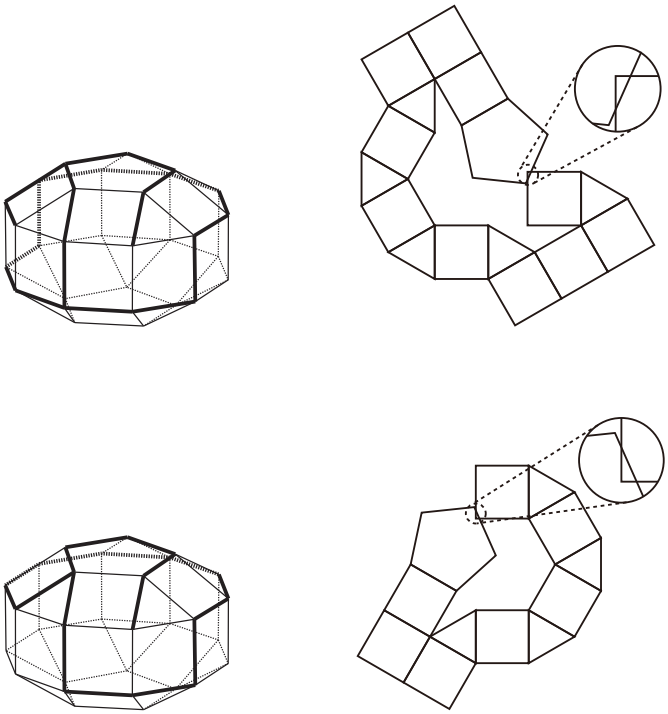

Figure A.8: Overlapping edge unfoldings in an elongated pentagonal gyrobicupola (J38). The right edge unfoldings are obtained by cutting along the thick line of the left convex polyhedrons. It has no other types of overlapping edge unfoldings. (continue)

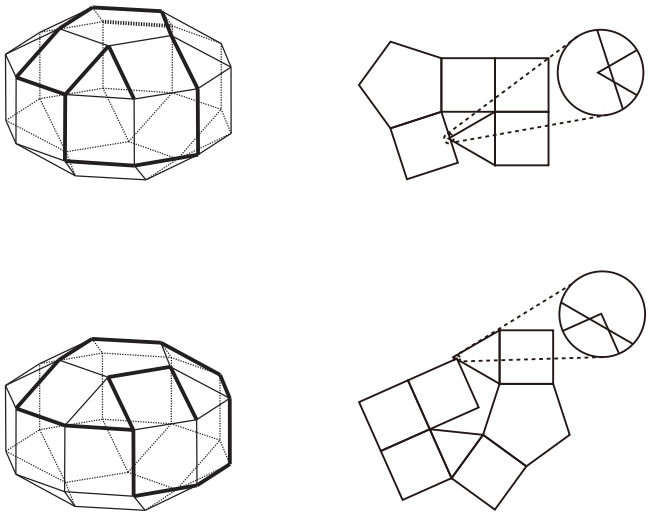

Figure A.9: Overlapping edge unfoldings in an elongated pentagonal gyrobicupola (J39). The right edge unfoldings are obtained by cutting along the thick line of the left convex polyhedrons. It has no other types of overlapping edge unfoldings.

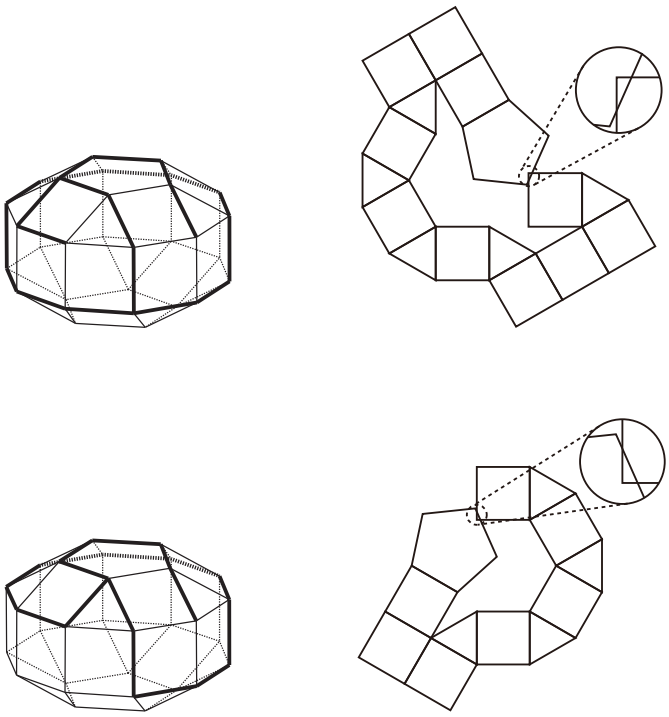

Figure A.9: Overlapping edge unfoldings in an elongated pentagonal gyrobicupola (J39). The right edge unfoldings are obtained by cutting along the thick line of the left convex polyhedrons. It has no other types of overlapping edge unfoldings. (continue)

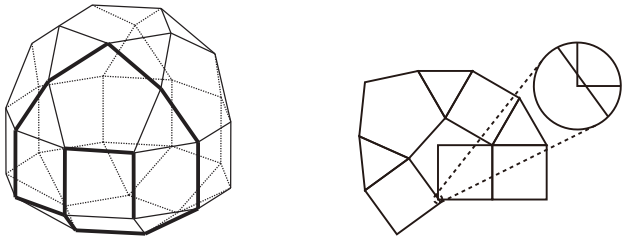

Figure A.10: An verlapping edge unfolding in an elongated pentagonal orthocupolarotunda (J40). The right edge unfoldings are obtained by cutting along the thick line of the left convex polyhedrons.

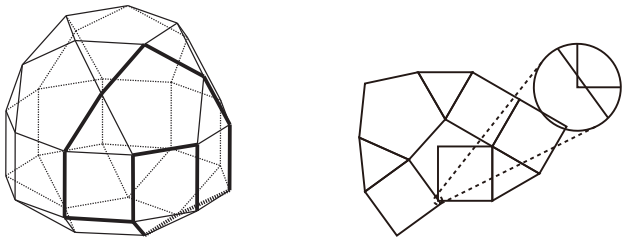

Figure A.11: An verlapping edge unfolding in an elongated pentagonal gyrocupolarotunda (J41). The right edge unfoldings are obtained by cutting along the thick line of the left convex polyhedrons.

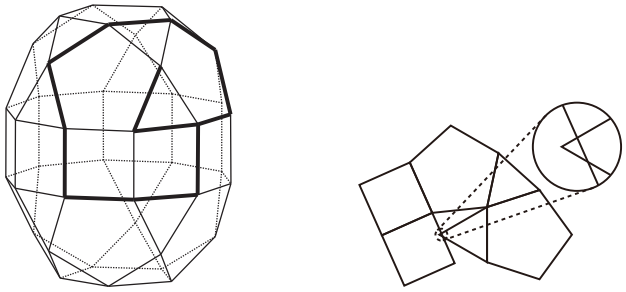

Figure A.12: An verlapping edge unfolding in an elongated pentagonal orthobirotunda (J42). The right edge unfoldings are obtained by cutting along the thick line of the left convex polyhedrons.

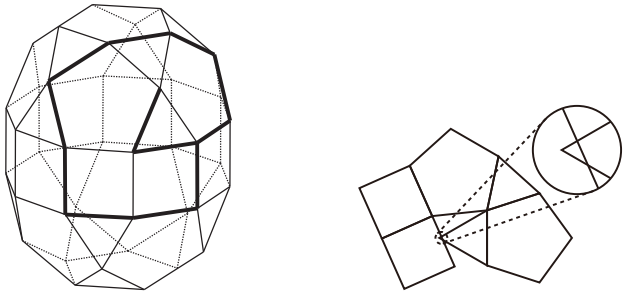

Figure A.13: An overlapping edge unfoldings in an elongated pentagonal gyrobirotunda (J43). The right edge unfoldings are obtained by cutting along the thick line of the left convex polyhedrons.

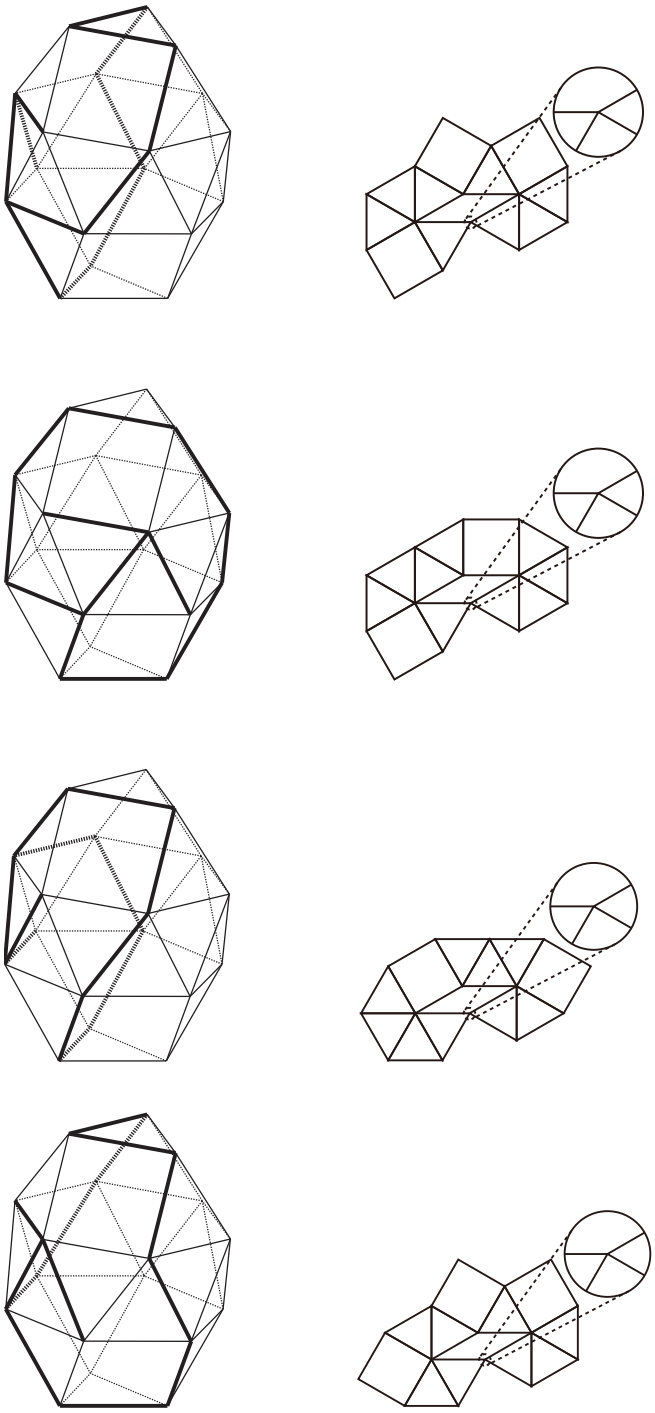

Figure A.14: Overlapping edge unfoldings in a gyroelongated triangular bicupola (J44). The right edge unfoldings are obtained by cutting along the thick line of the left convex polyhedrons. It has no other types of overlapping edge unfoldings.

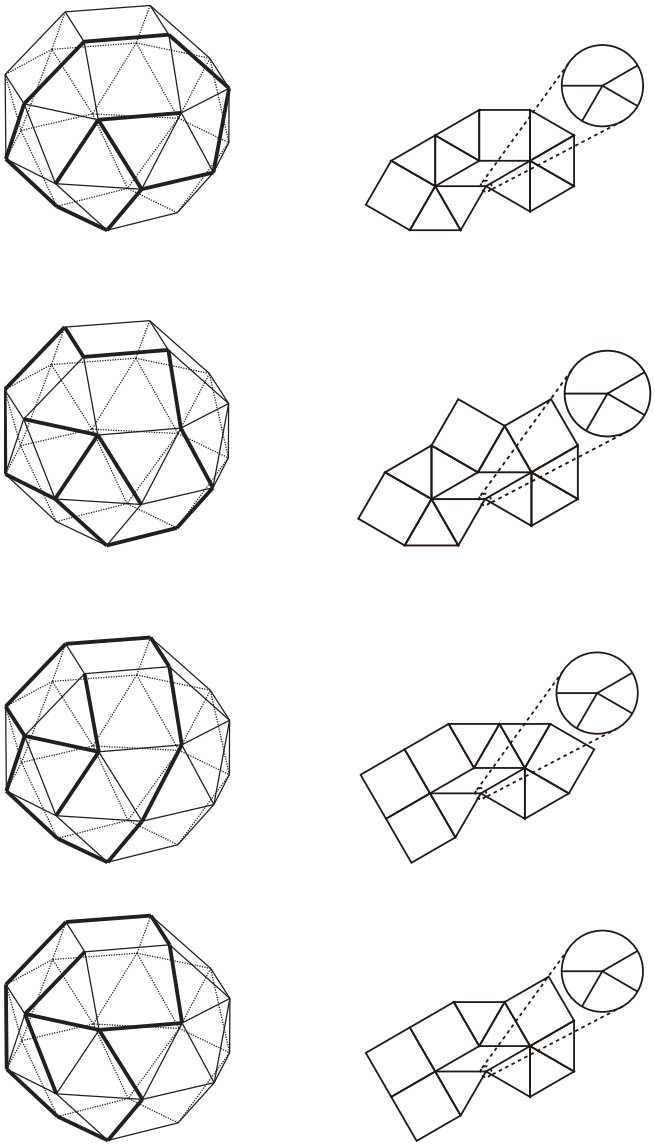

Figure A.15: Overlapping edge unfoldings in a gyroelongated square bicupola (J45). The right edge unfoldings are obtained by cutting along the thick line of the left convex polyhedrons. It has no other types of overlapping edge unfoldings.

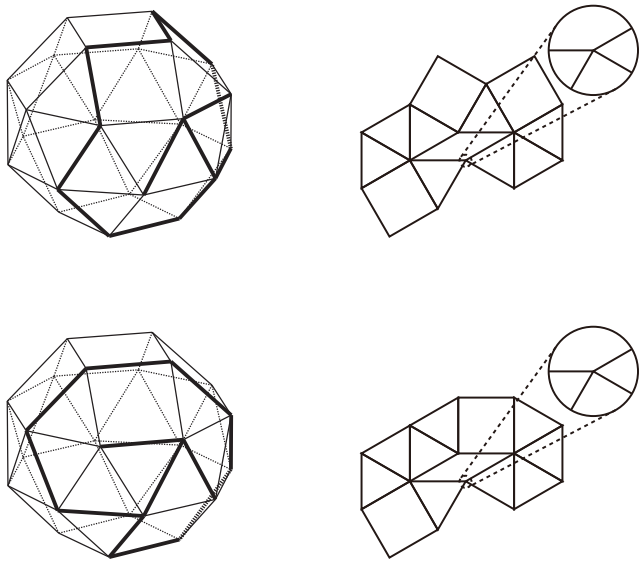

Figure A.15: Overlapping edge unfoldings in a gyroelongated square bicupola (J45). The right edge unfoldings are obtained by cutting along the thick line of the left convex polyhedrons. It has no other types of overlapping edge unfoldings. (continue)

Figure A.16: An overlapping edge unfoldings in a gyroelongated pentagonal bicupola (J46). The right edge unfoldings are obtained by cutting along the thick line of the left convex polyhedrons.

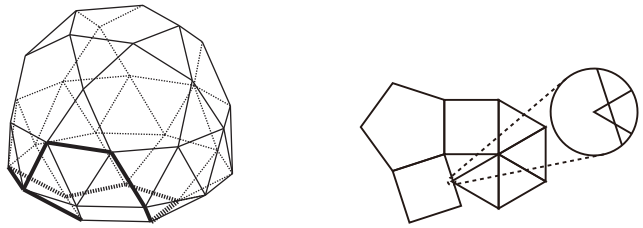

Figure A.17: An overlapping edge unfoldings in a gyroelongated pentagonal cupolarotunda (J47). The right edge unfoldings are obtained by cutting along the thick line of the left convex polyhedrons.

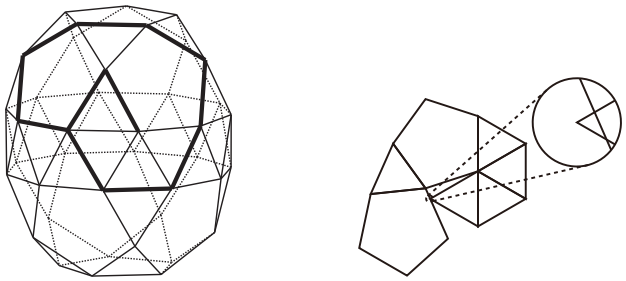

Figure A.18: An overlapping edge unfoldings in a gyroelongated pentagonal birotunda (J48). The right edge unfoldings are obtained by cutting along the thick line of the left convex polyhedrons.

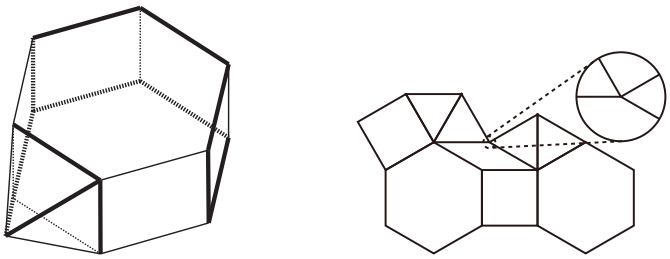

Figure A.19: An verlapping edge unfolding in an augmented hexagonal prism (J54). The right edge unfoldings are obtained by cutting along the thick line of the left convex polyhedrons. It has no other types of overlapping edge unfoldings.

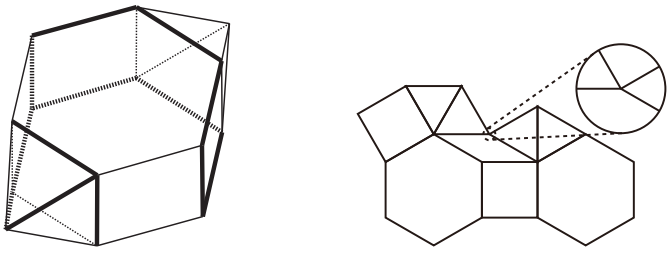

Figure A.20: An verlapping edge unfolding in a parabiaugmented hexagonal prism (J55). The right edge unfoldings are obtained by cutting along the thick line of the left convex polyhedrons. It has no other types of overlapping edge unfoldings.

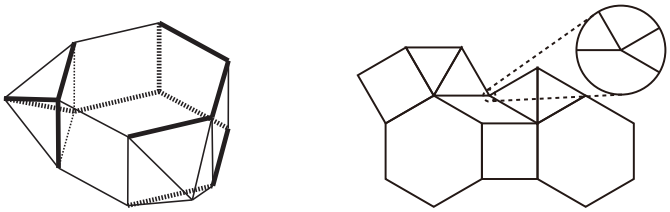

Figure A.21: An verlapping edge unfolding in a metabiaugmented hexagonal prism (J56). The right edge unfoldings are obtained by cutting along the thick line of the left convex polyhedrons. It has no other types of overlapping edge unfoldings.

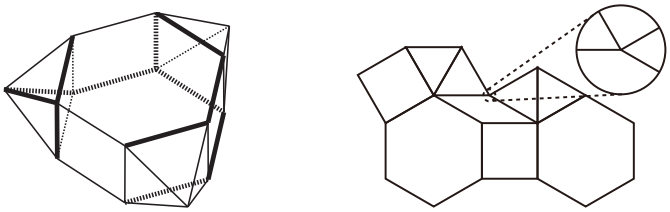

Figure A.22: An verlapping edge unfolding in a triaugmented hexagonal prism (J57). The right edge unfoldings are obtained by cutting along the thick line of the left convex polyhedrons. It has no other types of overlapping edge unfoldings.

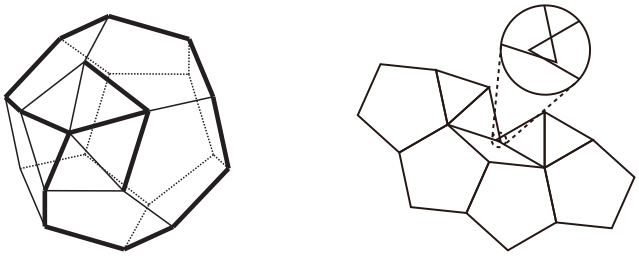

Figure A.23: An verlapping edge unfolding in an augmented dodecahedron (J58). The right edge unfoldings are obtained by cutting along the thick line of the left convex polyhedrons. It has no other types of overlapping edge unfoldings.

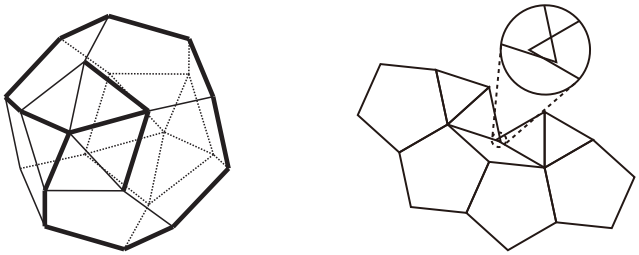

Figure A.24: An verlapping edge unfolding in a parabiaugmented dodecahedron (J59). The right edge unfoldings are obtained by cutting along the thick line of the left convex polyhedrons. It has no other types of overlapping edge unfoldings.

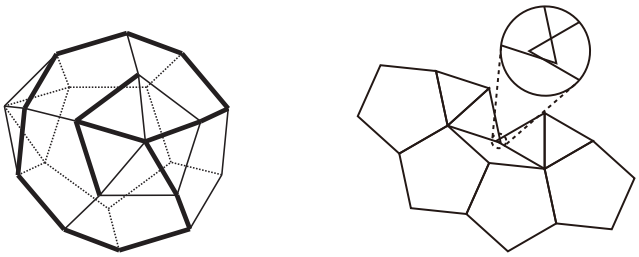

Figure A.25: An verlapping edge unfolding in a metabiaugmented dodecahedron (J60). The right edge unfoldings are obtained by cutting along the thick line of the left convex polyhedrons. It has no other types of overlapping edge unfoldings.

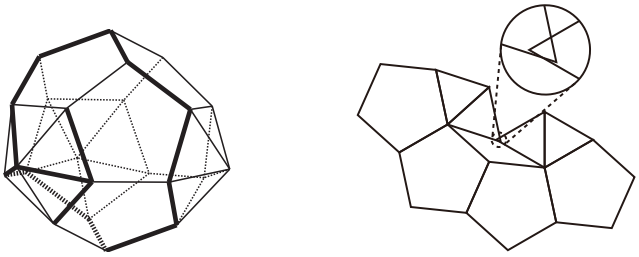

Figure A.26: An verlapping edge unfolding in a triaugmented dodecahedron (J61). The right edge unfoldings are obtained by cutting along the thick line of the left convex polyhedrons. It has no other types of overlapping edge unfoldings.

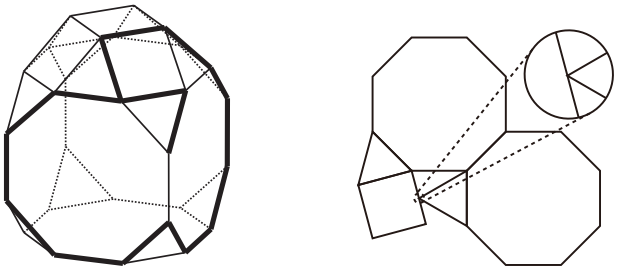

Figure A.27: Overlapping edge unfoldings in an augmented truncated cube (J66). The right edge unfoldings are obtained by cutting along the thick line of the left convex polyhedrons. It has no other types of overlapping edge unfoldings.

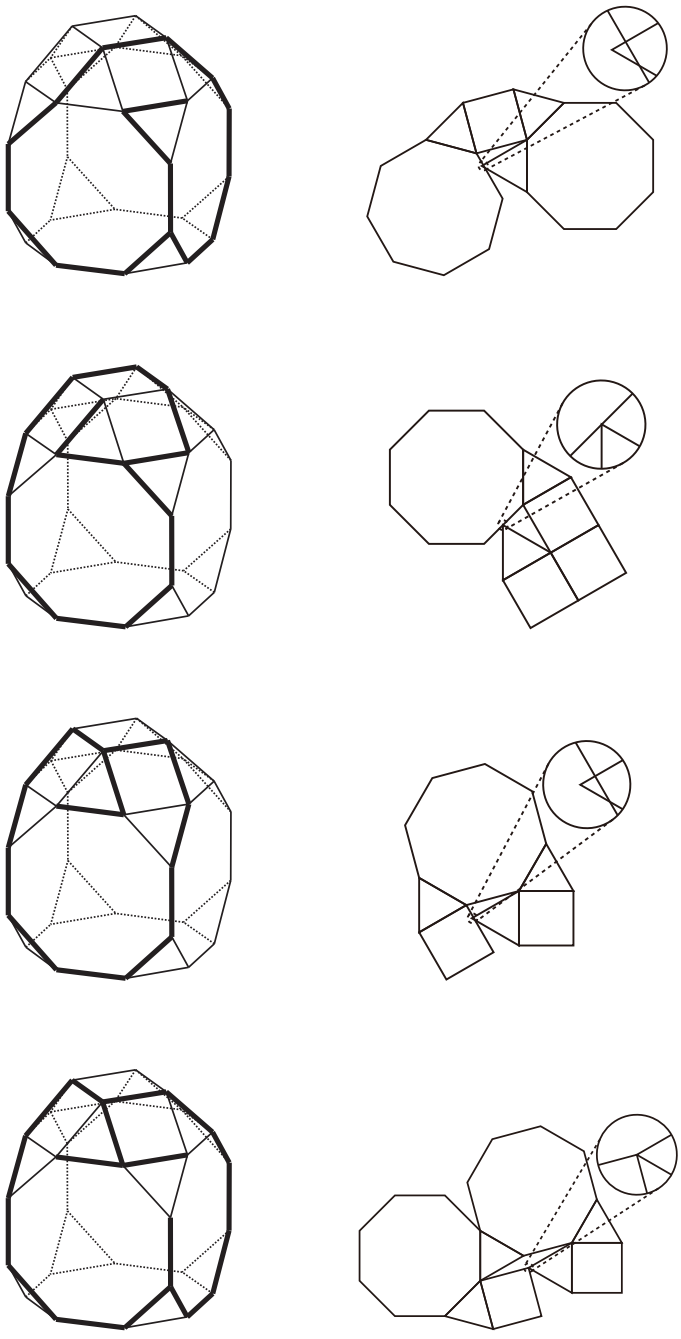

Figure A.27: Overlapping edge unfoldings in an augmented truncated cube (J66). The right edge unfoldings are obtained by cutting along the thick line of the left convex polyhedrons. It has no other types of overlapping edge unfoldings. (continue)

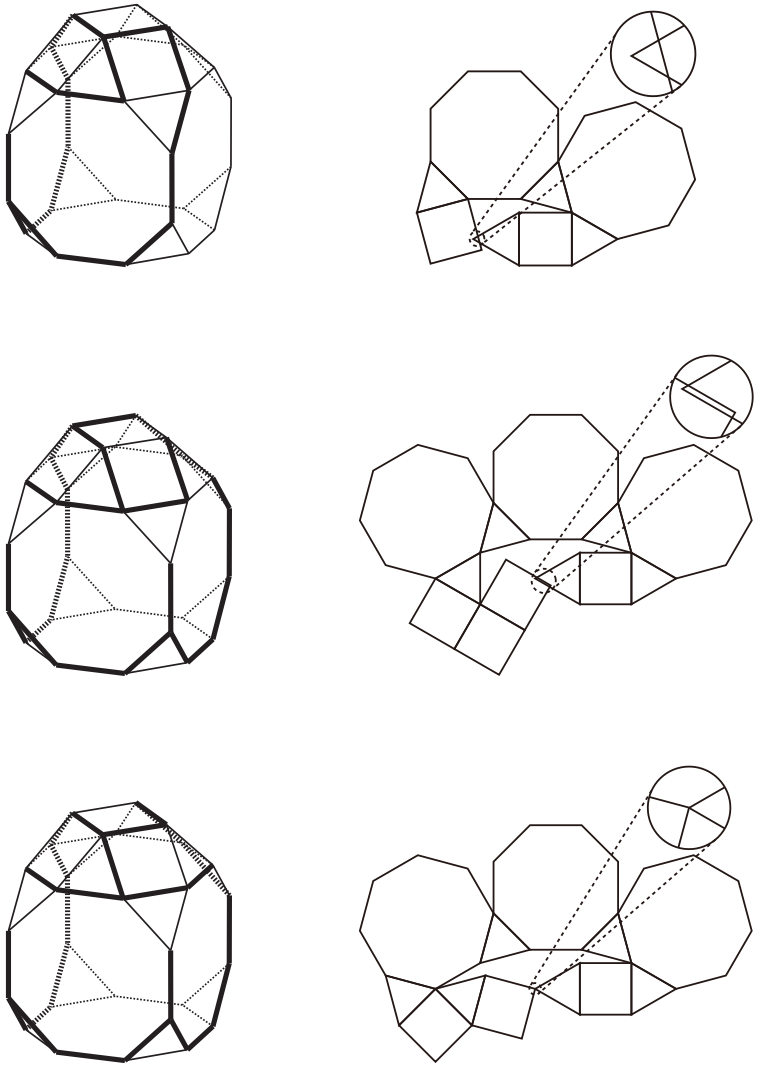

Figure A.27: Overlapping edge unfoldings in an augmented truncated cube (J66). The right edge unfoldings are obtained by cutting along the thick line of the left convex polyhedrons. It has no other types of overlapping edge unfoldings. (continue)

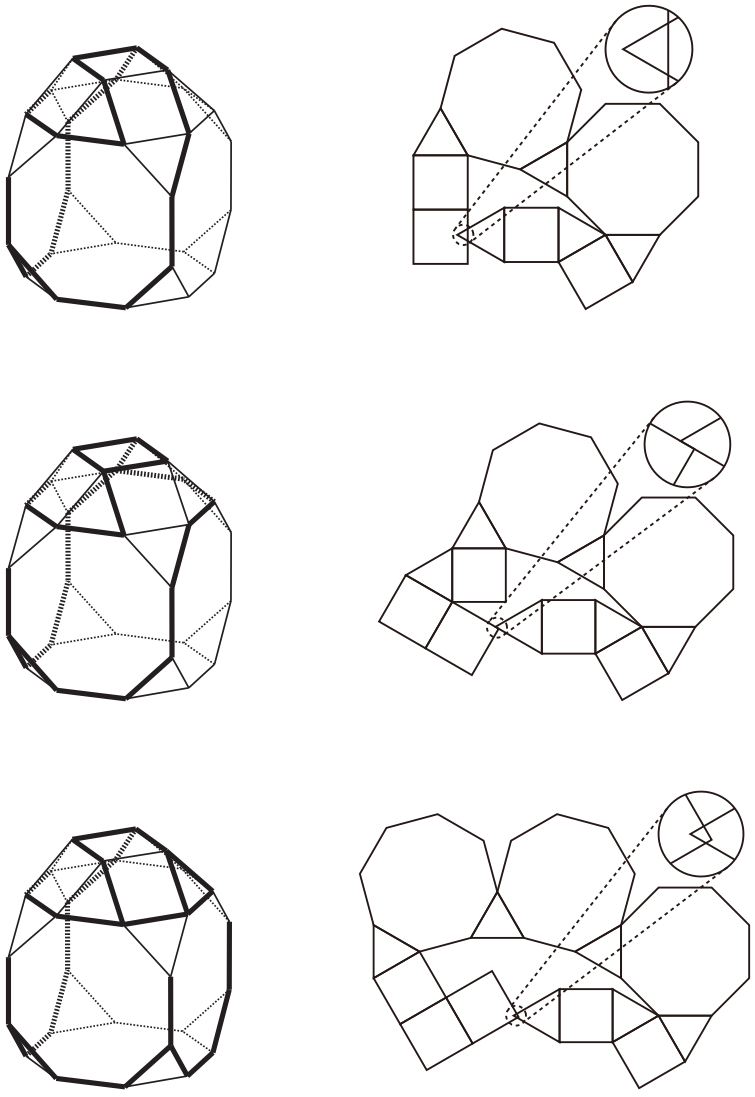

Figure A.27: Overlapping edge unfoldings in an augmented truncated cube (J66). The right edge unfoldings are obtained by cutting along the thick line of the left convex polyhedrons. It has no other types of overlapping edge unfoldings. (continue)

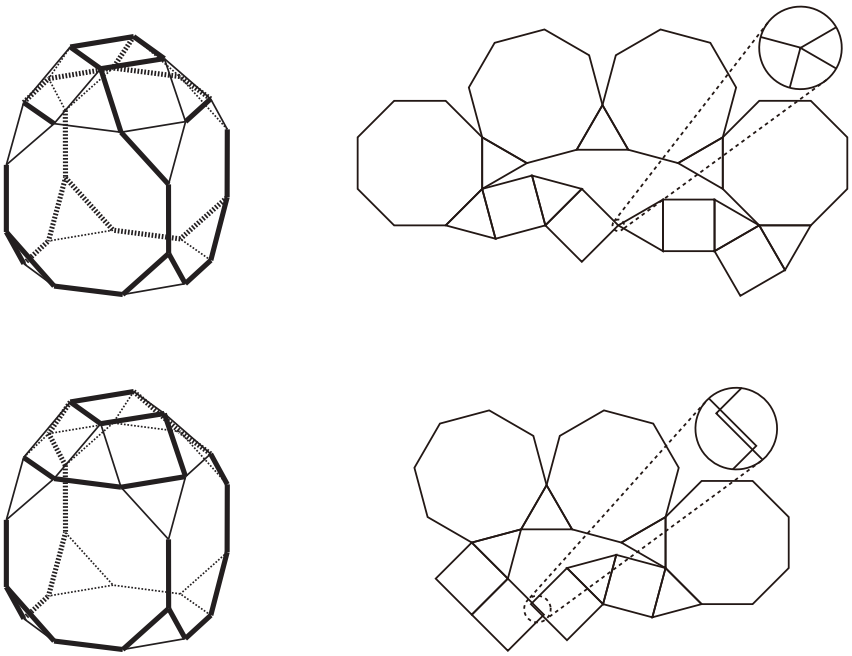

Figure A.27: Overlapping edge unfoldings in an augmented truncated cube (J66). The right edge unfoldings are obtained by cutting along the thick line of the left convex polyhedrons. It has no other types of overlapping edge unfoldings. (continue)

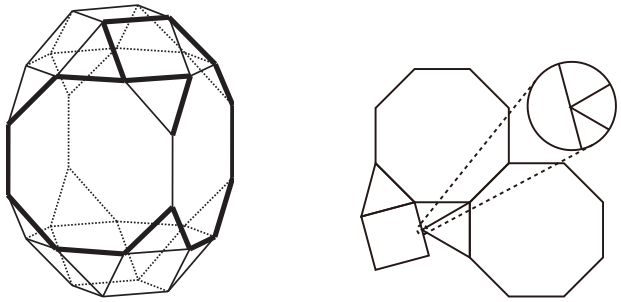

Figure A.28: Overlapping edge unfoldings in a biaugmented truncated cube (J67). The right edge unfoldings are obtained by cutting along the thick line of the left convex polyhedrons. It has no other types of overlapping edge unfoldings.

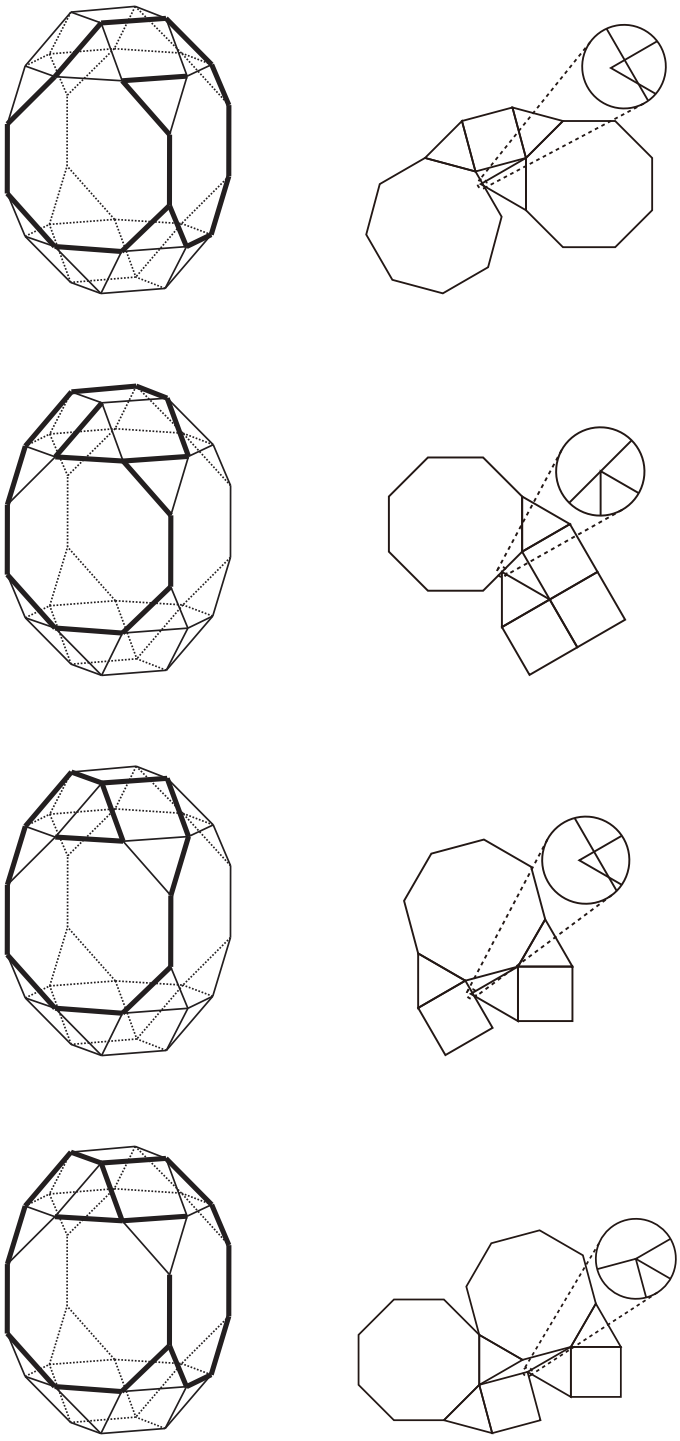

Figure A.28: Overlapping edge unfoldings in a biaugmented truncated cube (J67). The right edge unfoldings are obtained by cutting along the thick line of the left convex polyhedrons. It has no other types of overlapping edge unfoldings. (continue)

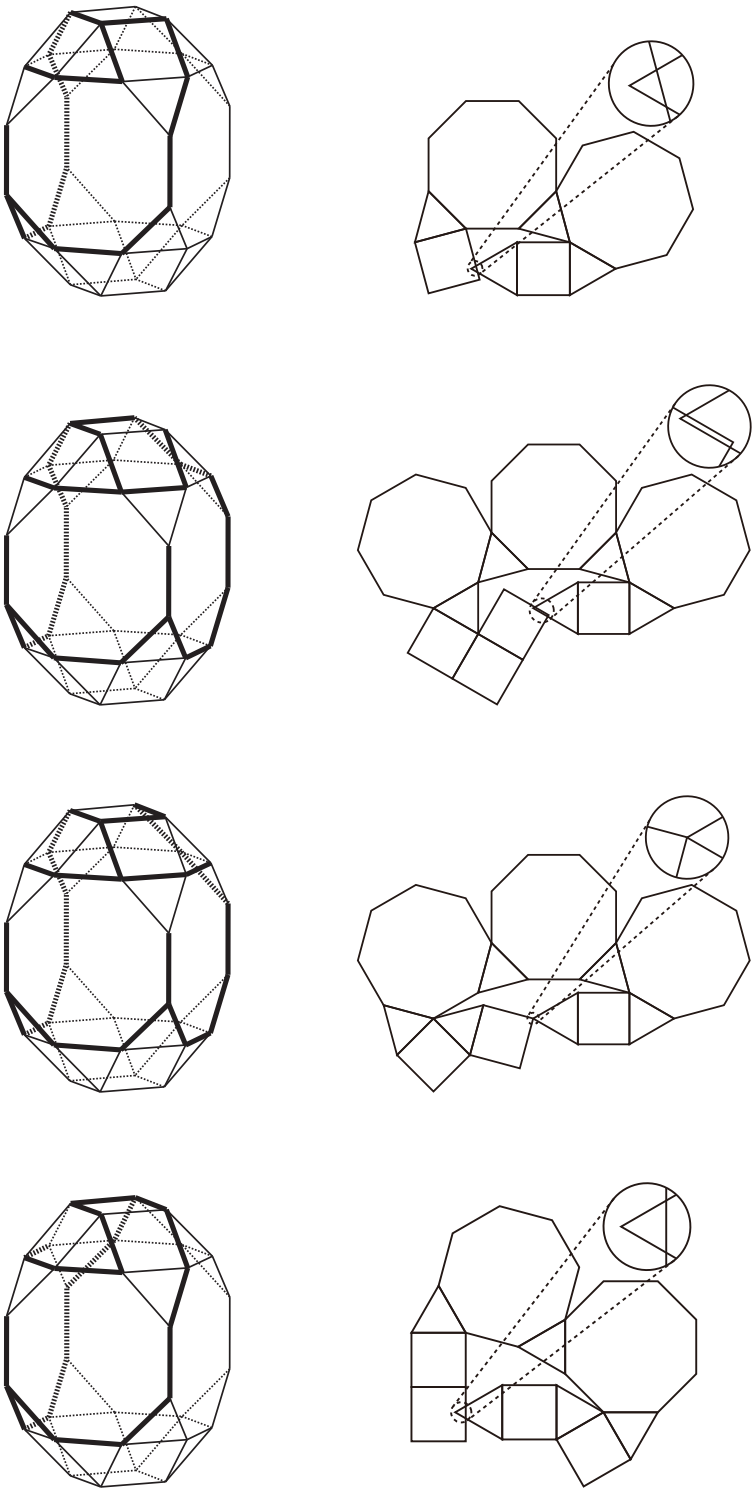

Figure A.28: Overlapping edge unfoldings in a biaugmented truncated cube (J67). The right edge unfoldings are obtained by cutting along the thick line of the left convex polyhedrons. It has no other types of overlapping edge unfoldings. (continue)

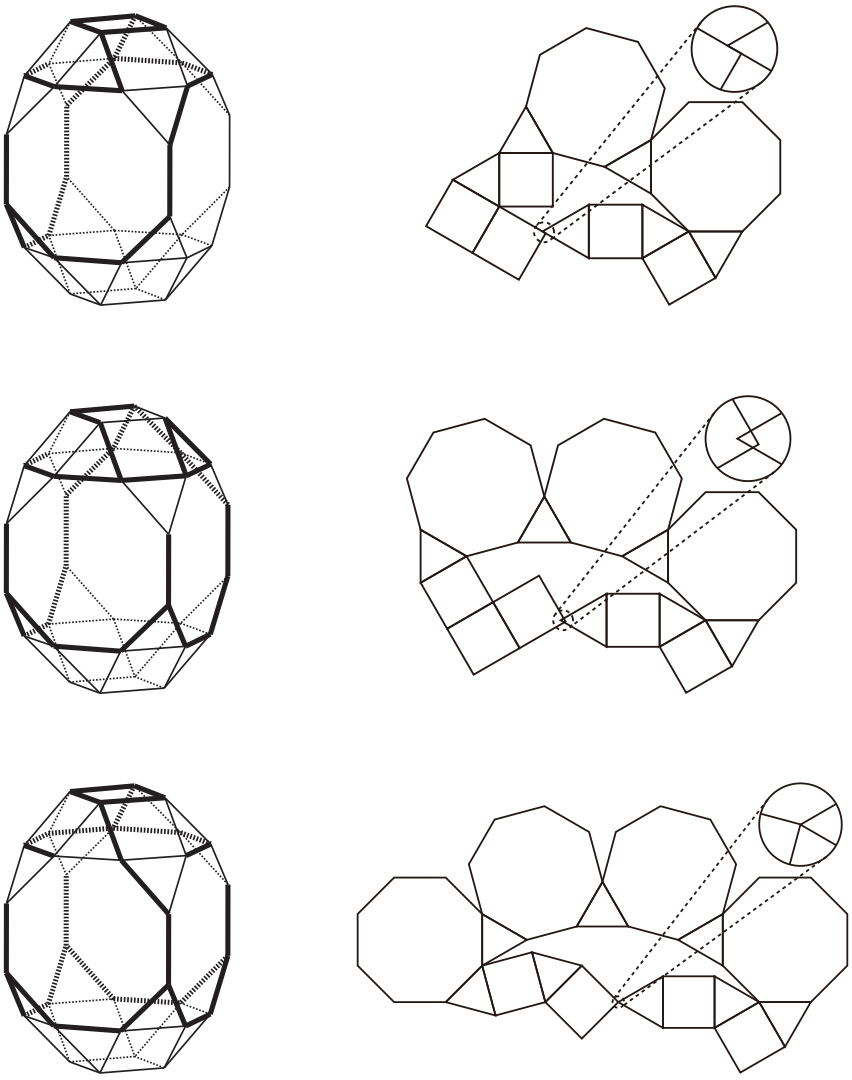

Figure A.28: Overlapping edge unfoldings in a biaugmented truncated cube (J67). The right edge unfoldings are obtained by cutting along the thick line of the left convex polyhedrons. It has no other types of overlapping edge unfoldings. (continue)

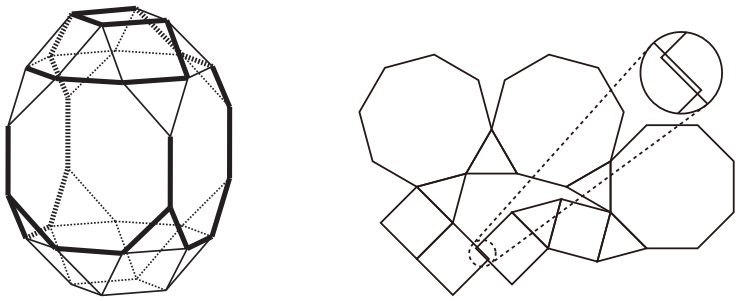

Figure A.28: Overlapping edge unfoldings in a biaugmented truncated cube (J67). The right edge unfoldings are obtained by cutting along the thick line of the left convex polyhedrons. It has no other types of overlapping edge unfoldings. (continue)

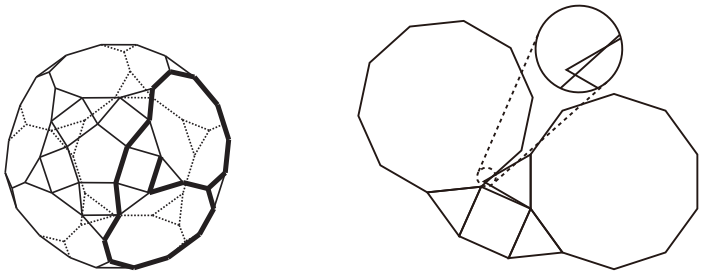

Figure A.29: An overlapping edge unfoldings in an augmented truncated dodecahedron (J68). The right edge unfoldings are obtained by cutting along the thick line of the left convex polyhedrons.

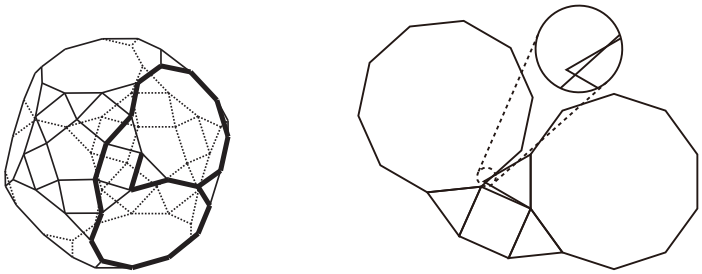

Figure A.30: An overlapping edge unfoldings in a parabiaugmented truncated dodecahedron (J69). The right edge unfoldings are obtained by cutting along the thick line of the left convex polyhedrons.

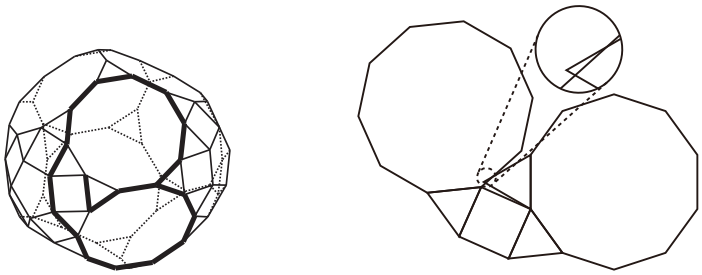

Figure A.31: An overlapping edge unfoldings in a metabiaugmented truncated dodecahedron (J70). The right edge unfoldings are obtained by cutting along the thick line of the left convex polyhedrons.

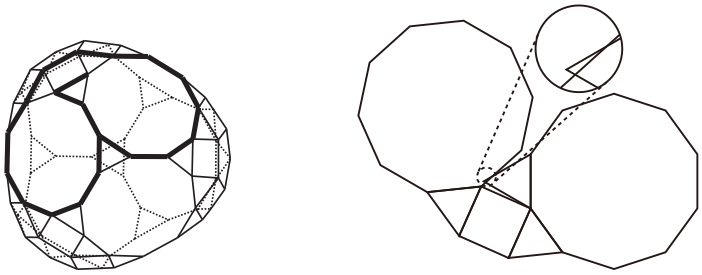

Figure A.32: An overlapping edge unfoldings in a triaugmented truncated dodecahedron (J71). The right edge unfoldings are obtained by cutting along the thick line of the left convex polyhedrons.

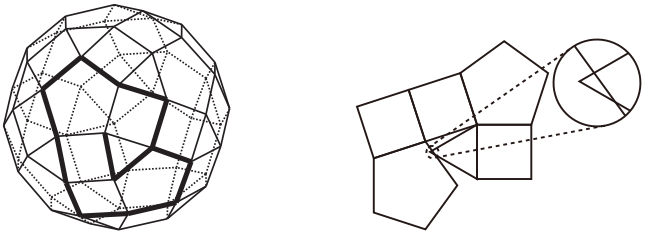

Figure A.33: An overlapping edge unfoldings in a gyrate rhombicosidodecahedron (J72). The right edge unfoldings are obtained by cutting along the thick line of the left convex polyhedrons.

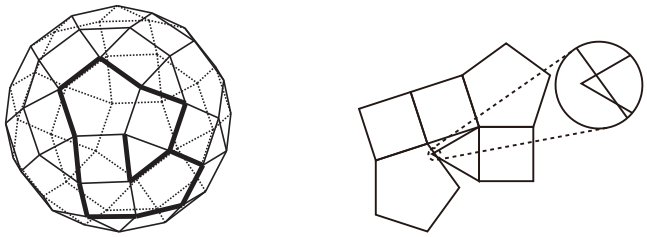

Figure A.34: An overlapping edge unfoldings in a parabigyrate rhombicosidodecahedron (J73). The right edge unfoldings are obtained by cutting along the thick line of the left convex polyhedrons.

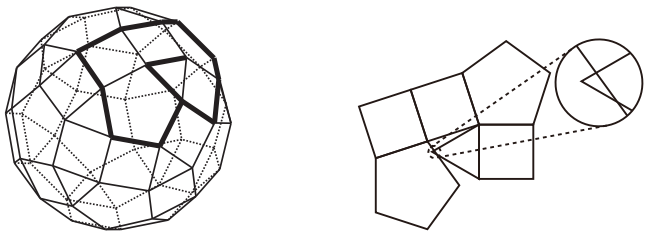

Figure A.35: An overlapping edge unfoldings in a metabigyrate rhombicosidodecahedron (J74). The right edge unfoldings are obtained by cutting along the thick line of the left convex polyhedrons.

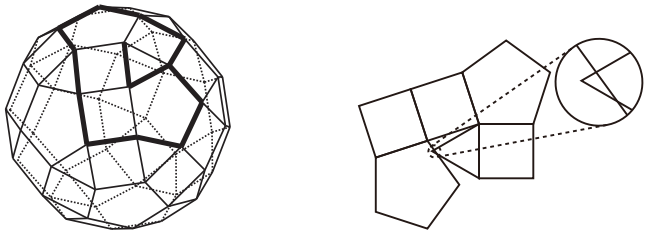

Figure A.36: An overlapping edge unfoldings in a trigyrate rhombicosidodecahedron (J75). The right edge unfoldings are obtained by cutting along the thick line of the left convex polyhedrons.

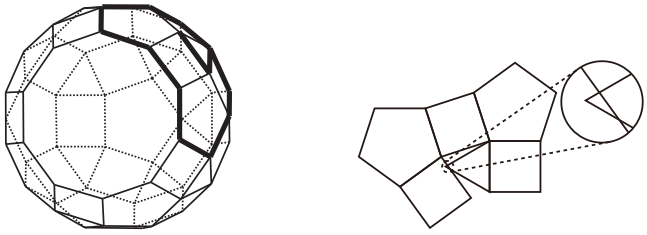

Figure A.37: An overlapping edge unfoldings in a diminished rhombicosidodecahedron (J76). The right edge unfoldings are obtained by cutting along the thick line of the left convex polyhedrons.

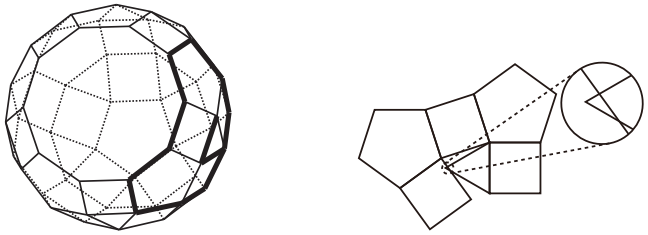

Figure A.38: An overlapping edge unfoldings in a paragyrate diminished rhombicosidodecahedron (J77). The right edge unfoldings are obtained by cutting along the thick line of the left convex polyhedrons.

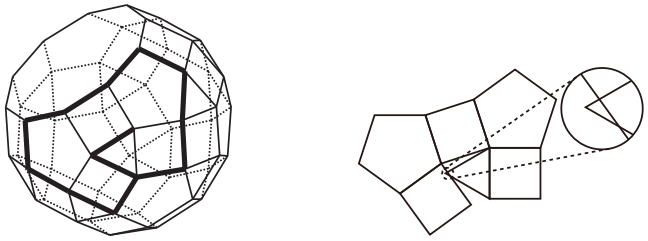

Figure A.39: An overlapping edge unfoldings in a metagyrate diminished rhombicosidodecahedron (J78). The right edge unfoldings are obtained by cutting along the thick line of the left convex polyhedrons.

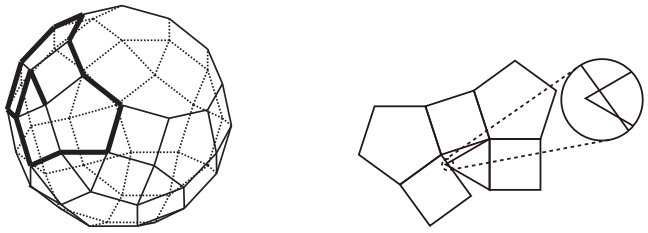

Figure A.40: An overlapping edge unfoldings in a bigyrate diminished rhombicosidodecahedron (J79). The right edge unfoldings are obtained by cutting along the thick line of the left convex polyhedrons.

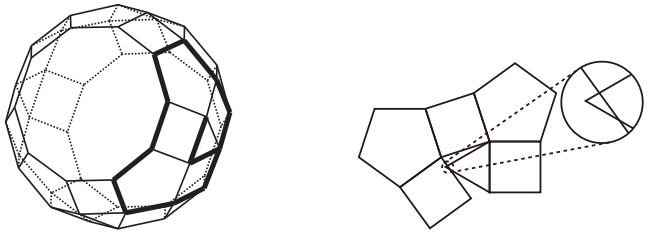

Figure A.41: An overlapping edge unfoldings in a parabidiminished rhombicosidodecahedron (J80). The right edge unfoldings are obtained by cutting along the thick line of the left convex polyhedrons.

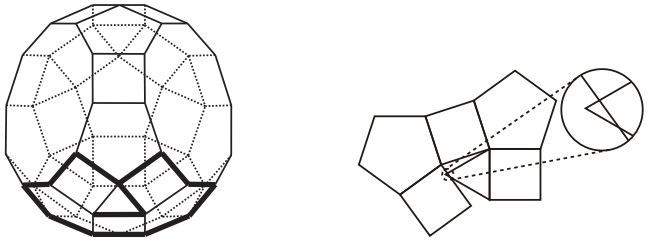

Figure A.42: An overlapping edge unfoldings in a metabidiminished rhombicosidodecahedron (J81). The right edge unfoldings are obtained by cutting along the thick line of the left convex polyhedrons.

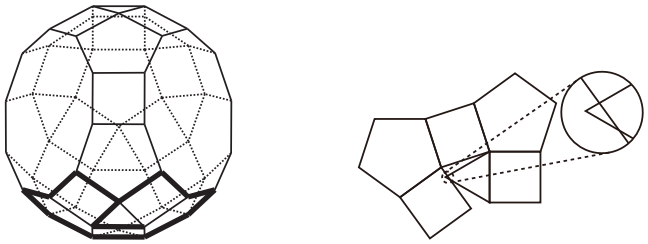

Figure A.43: An overlapping edge unfoldings in a gyrate bidiminished rhombicosidodecahedron (J82). The right edge unfoldings are obtained by cutting along the thick line of the left convex polyhedrons.

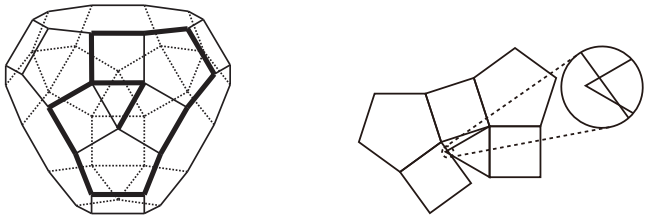

Figure A.44: An overlapping edge unfoldings in a tridiminished rhombicosidodecahedron (J83). The right edge unfoldings are obtained by cutting along the thick line of the left convex polyhedrons.

Publications

Refereed International Conference

[1] Takumi Shiota and Toshiki Saitoh: "Overlapping Edge Unfoldings for Archimedean Solids and (Anti)prisms", The 17th International Conference and Workshop on Algorithms and Computation (WALCOM 2023), Lecture Notes in Computer Science, to appear, March 22–24, 2023, Hsinchu (Taiwan) and online.

Domestic Workshops (No peer review)

[2] 塩田拓海，斎藤寿樹: "回転展開法を用いた自己重複を持つ部分的な辺展開図の数え上げ"，2021 年度 夏の LA シンポジウム，pp.3:1-8, 2021 年 7 月 20-21 日，オンライン.

[3] 塩田拓海，斎藤寿樹: "回転展開法を用いた自己重複を持つ部分的な辺展開図の数え上げ"，2021 年度（第 74 回）電気・情報関係学会九州支部連合大会, 06-1A-10, pp.1–2, 2021 年 9 月 24-25 日, オンライン.

[4] 塩田拓海，斎藤寿樹: "アルキメデスの角柱の重なりを持つ辺展開図"，日本オペレーションズ・リサーチ学会九州支部若手 OR 交流会 2021，2021 年 11 月 13 日, オンライン.

[5] 塩田拓海，斎藤寿樹: "アルキメデスの（反）角柱の重なりを持つ辺展開図"，2021 年度 冬の LA シンポジウム，pp.5:1-11，2022 年 2 月 1-3 日，オンライン.

[6] 塩田拓海: "凸多面体の重なりを持つ辺展開図の列挙"，第 3 回 AFSA B01 セミナー SSSS, 2022 年 7 月 30 日-8 月 1 日，TKP ガーデンシティ PREMIUM 札幌大通り（北海道）.

[7] 塩田拓海，鎌田斗南，上原隆平: "立方体の格子展開図における重なり"，日本オペレーションズ・リサーチ学会九州支部 若手 OR 交流会 2022, 2022 年 10 月 29 日，福岡大学（福岡）.

[8] 有吉優聖，塩田拓海，斎藤寿樹: “タンパク質連接ネットワークの中心性とランダムコイル指標の関係”，日本オペレーションズ・リサーチ学会九州支部 若手 OR 交流会 2022，2022 年 10 月 29 日，福岡大学（福岡）.

[9] 塩田拓海，鎌田斗南，上原隆平: “直方体の格子展開図における重なり”，2022 年度冬の LA シンポジウム，pp.9:1-12，2023 年 1 月 30 日-2 月 1 日，京都大学（京都）.

Awards

[10] 2021 年 9 月 2021 年度 (第 74 回) 電気・情報関係学会九州支部連合大会 連合大会講演奨励賞

[11] 2021 年 11 月 日本オペレーションズ・リサーチ学会九州支部 若手 OR 交流会 2021 優秀発表賞

[12] 2022 年 10 月 日本オペレーションズ・リサーチ学会九州支部 若手 OR 交流会 2022 優秀発表賞